# Geometry and Topology of Waves in Soft and Structured Matter

2026 Boulder Summer School for Condensed Matter Physics Lecture Notes

[**Xiaoming's note: This is a preliminary version. I'm still adding references and making edits. I will update this file by the time of the lecture. **]

## Contents

# Lecture 1: Multiscale Physics of Waves in Soft and Structured Matter

**Overview.** Wave propagation is a universal phenomenon, but the physics involved change dramatically across length scales. This lecture first surveys wave phenomena across soft matter scales—from atomic crystals and soft bulk configurations to fluid interfaces and architected metamaterials—and formulate their governing scalar and vector wave equations. We then expose the limitations of idealized wave theory by exploring the "hidden physics" in soft and structured matter: nonlinearity, dissipation, viscoelasticity, disorder, microstructure, and internal resonances. Finally, we focus on spatial periodicity—a common feature in soft and structured matter—establishing how Bragg scattering opens up band gaps and how Bloch's theorem describes waves in periodic systems using reciprocal lattices and Brillouin zones, preparing us for wave geometry and topology in Lectures 2 and 3.

## 1.1. Waves in soft matter across scales

You see wave equations everywhere in physics. They can be generally written as

$$\partial_t^2 u = c^2 \nabla^2 u. \tag{1.1.1}$$

Here $u(\boldsymbol{r}, t)$ is a field and $c$ is a wave speed.

Where is this equation from? In introductory courses you may have derived it from equations of motion of coupled oscillators or Maxwell equations. In advanced courses you may have derived it from the Lagrangian of a field theory.

**Homework connection.** The homework derives this equation from a Lagrangian density. This gives a more systematic way to see how conservative dynamics, shift symmetry, and gradient elasticity lead to the ideal wave equation.

However, except for a few special cases, such as electromagnetic waves or gravitational waves, wave equations are usually *effective long-wavelength descriptions of collective degrees of freedom.*

This is especially true in soft matter systems, which involve a rich collection of different dynamics and emergent degrees of freedom across scales. Here is a table summarizing some aspects of this,

| **Length scale** | **Example systems** | **Propagating field** | **Restoring force** |
|---|---|---|---|
| Å–nm | Atomic crystals | Atomic displacement | Interatomic bonds |
| nm–$\mu$m | **Bulk soft matter**: nanoparticles, colloids, polymers, gels, foams, liquid crystals | Density, displacement, orientation | Entropy and interactions |
| nm–$\mu$m | **Surface soft matter**: membranes, interfaces | Height or displacement field | Bending, tension, surface energy |
| $\mu$m–m | Phononic crystals, mechanical metamaterials | Displacement, pressure, strain | Elasticity, constraints |

This means that to describe waves in soft matter, we should bear in mind that coefficients in this equation are often not simple constants, but

- arise from complex multiscale interactions and entropy
- incorporates coarse-grained effects of entropy, disorder, and heterogeneity
- evolve over length scales due to renormalization

The purpose of this lecture is to discuss the wave equation in various systems and scales, especially focusing on bulk soft matter systems and metamaterials with periodic structures.

## 1.2. Ideal scalar and vector wave equations

To discuss phenomena in soft matter that are explained by wave propagation, let's first do a brief review of wave equations in a few simple cases.

### 1.2.1. Scalar wave equation

Let $u(\boldsymbol{r}, t)$ be a scalar displacement-like field. The wave equation can be generally written as

$$\rho \partial_t^2 u = K \nabla^2 u, \tag{1.2.1}$$

where $\rho$ is an inertial coefficient and $K$ is a stiffness. Real mechanical waves are described by vector displacement fields, and only obey this equation in special limits, but it is useful to start from this scalar equation to lay out the foundation.

Equivalently,

$$\partial_t^2 u = c^2 \nabla^2 u, \qquad c^2 = \frac{K}{\rho}, \tag{1.2.2}$$

where $c$ is the speed of the wave.

This equation is supported by the system being homogeneous, isotropic, inversion symmetric, and time-reversal symmetric, as well as a translation symmetry

$$u \to u + \text{constant}. \tag{1.2.3}$$

If this symmetry is broken, e.g., by local pinning, we have

$$\rho \partial_t^2 u = K \nabla^2 u - \kappa u. \tag{1.2.4}$$

General solutions to these equations can be written as planewaves

$$u(\boldsymbol{r}, t) = u_0 e^{i(\mathbf{k}\cdot\mathbf{r} - \omega t)}. \tag{1.2.5}$$

Plug this into Eq. (1.2.2) we have

$$\omega = \pm ck, \tag{1.2.6}$$

the familiar linear dispersion relation. Plug this into Eq. (1.2.4) we have

$$\omega^2 = c^2 k^2 + \omega_0^2 \qquad \omega_0^2 = \frac{\kappa}{\rho}. \tag{1.2.7}$$

The $\omega_0$ term is often called a "mass term" or a "gap." This is because when you quantize these waves, following De Broglie relation, $\epsilon = \hbar\omega, p = \hbar k$, the dispersion relation becomes the energy momentum relation of a relativistic particle, $\epsilon = \sqrt{m^2 + c^2 p^2}$, with $\omega_0$ corresponding to the rest mass. Such gapped modes arise in many contexts, including optical phonons, local resonators, pinned elastic modes, and internal modes of metamaterials.

> **Homework connection.** One homework question asks what changes in the equation of motion and dispersion relation when this shift symmetry is broken by a pinning term.

### 1.2.2. Vector wave equation

For an elastic solid in 3D, the field is a displacement vector

$$\boldsymbol{u}(\boldsymbol{r}, t) = (u_x, u_y, u_z). \tag{1.2.8}$$

The equation of motion follows from momentum conservation:

$$\rho \partial_t^2 u_i = \partial_j \sigma_{ij}, \tag{1.2.9}$$

where $\sigma_{ij}$ is the stress tensor. In linear elasticity, as you learned from previous lectures

$$\sigma_{ij} = C_{ijkl} u_{kl}, \qquad u_{kl} = \frac{1}{2}(\partial_k u_l + \partial_l u_k), \tag{1.2.10}$$

where $u_{kl}$ is the linear strain tensor and $C_{ijkl}$ is the elastic constant tensor.

For an isotropic solid,

$$\sigma_{ij} = \lambda \delta_{ij} u_{kk} + 2\mu u_{ij}, \tag{1.2.11}$$

where $\lambda$ and $\mu$ are the Lame coefficients. The equation of motion becomes

$$\rho \partial_t^2 \boldsymbol{u} = (\lambda + \mu) \nabla(\nabla \cdot \boldsymbol{u}) + \mu \nabla^2 \boldsymbol{u}. \tag{1.2.12}$$

We can also write the sub indices explicitly and have

$$\rho\, \partial_t^2 u_i = (\lambda + \mu)\, \partial_i \partial_j u_j + \mu\, \partial_j \partial_j u_i, \tag{1.2.13}$$

This equation naturally separates into longitudinal and transverse waves,

$$\boldsymbol{u} = \boldsymbol{u}_L + \boldsymbol{u}_T, \quad \text{with } \nabla \cdot \boldsymbol{u}_T = 0, \nabla \times \boldsymbol{u}_L = 0. \tag{1.2.14}$$

For a longitudinal wave, $\boldsymbol{u}$ is parallel to $\boldsymbol{k}$, and

$$\omega^2 = c_L^2 k^2, \qquad c_L^2 = \frac{\lambda + 2\mu}{\rho}. \tag{1.2.15}$$

For a transverse wave, $\boldsymbol{u}$ is perpendicular to $\boldsymbol{k}$, and

$$\omega^2 = c_T^2 k^2, \qquad c_T^2 = \frac{\mu}{\rho}. \tag{1.2.16}$$

Two interesting limits should be discussed here:

- $c_T = 0$: This is the case of ordinary fluids, which resist compression but do not support static shear stress. Therefore ordinary sound in a fluid is a longitudinal pressure or density wave.
- $c_L^2 = c_T^2 = \frac{\mu}{\rho}$ in 2D (conformal limit): In two dimensions, the displacement field is $\mathbf{u} = (u_x, u_y)$, and the indices $i, j, k$ run only over $x, y$. The isotropic elastic law has the same form,

  $$\sigma_{ij} = \lambda \delta_{ij} u_{kk} + 2\mu u_{ij},$$

  but the bulk modulus is now

  $$B_{\mathrm{2D}} = \lambda + \mu.$$

  Thus the limit $B_{\mathrm{2D}} = 0$ corresponds to $\lambda + \mu = 0$, which is the extreme auxetic limit with Poisson ratio $\nu = -1$. In this case the equation of motion reduces to the simple vector Laplacian form $\rho \partial_t^2 \mathbf{u} = \mu \nabla^2 \mathbf{u}$. The longitudinal and transverse waves become degenerate,

  $$c_L^2 = c_T^2 = \frac{\mu}{\rho}.$$

  This allows exotic phenomena such as backscattering free propagation of edge waves. This special case is specific to two dimensions; in three dimensions $B_{\mathrm{3D}} = \lambda + 2\mu/3$, so $B_{\mathrm{3D}} = 0$ does not give a pure Laplacian equation.

### 1.2.3. Interfaces, membranes, and plates

Soft matter often involves interfaces and thin structures, where geometry changes the form of the wave equation.

Consider a simple case of a solid thin plate, as introduced in earlier lectures. Let $h(x, y, t)$ be a height field describing an interface or membrane. The elastic energy can be written as

$$E[h] = \frac{1}{2} \int d^2 r \, \kappa (\nabla^2 h)^2. \tag{1.2.17}$$

The equation of motion takes the schematic form

$$\rho \partial_t^2 h = -\kappa \nabla^4 h, \tag{1.2.18}$$

so that

$$\omega^2 \sim k^4, \qquad \omega \sim k^2. \tag{1.2.19}$$

This is not the ordinary wave equation. The dispersion reflects the geometric cost of bending rather than stretching.

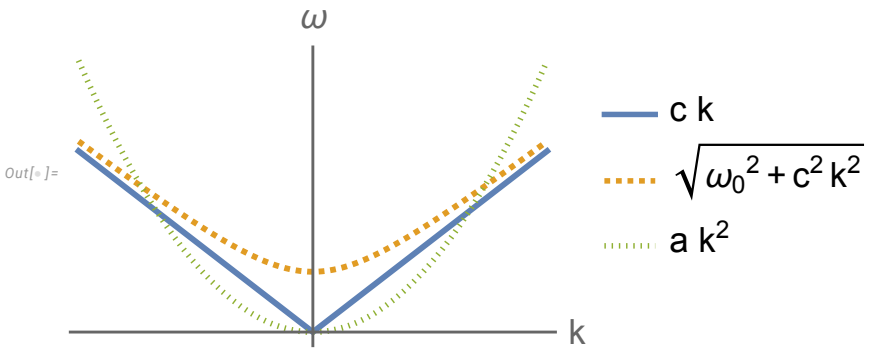


Figure 1: Dispersion relations of simple linear waves in homogeneous media with translation invariance $\omega = ck$, with local pinning $\omega = \sqrt{\omega_0^2 + c^2 k^2}$, and nonlinear dispersion due to thin geometry $\omega = ak^2$ (note that the wave is still linear).

### 1.2.4. Metamaterials

In metamaterials, the wave equation is shaped by the architecture by design: Hinges, beams, resonators, cavities, contacts, and constraints can all determine the effective dynamics.

A general form of elastic wave equation in metamaterials with internal structures can be schematically written as

$$\rho \partial_t^2 u_i = \partial_j \left( C_{ijkl}(\mathbf{r}) u_{kl} \right). \tag{1.2.20}$$

The geometry and topology of $C_{ijkl}(\mathbf{r})$ give us many ways to shape the wave dynamics! We will discuss this more extensively later.

## 1.3. Beyond ideal waves: hidden physics in soft and structured matter

The ideal wave equations we discussed above assumes linearity, locality, conservation, reciprocity, and deterministic dynamics. These assumptions are often violated in soft and structured matter, as we discussed in the beginning (Sec. 1.1). The following subsections describe common ways in which real systems go beyond this idealized form.

### 1.3.1. Nonlinearity

Linear wave equations assume small amplitudes and linear constitutive laws. Soft materials and metamaterials often involve large deformation, geometric nonlinearity, buckling, contact forces, and nonlinear elastic response. Instead of a linear stress-strain relation, one may have schematically

$$\sigma \sim \nabla u + (\nabla u)^2 + \cdots . \tag{1.3.1}$$

Consequences include amplitude-dependent wave speeds, harmonic generation, solitons, shocks, nonlinear localization, and deformation-dependent band structures.

A simple example is a chain of elastic beads, where Hertzian contact gives a nonlinear force law

$$F \sim \delta^{3/2}, \tag{1.3.2}$$

with $\delta$ the compression between neighboring beads. In such a system the propagation speed can depend strongly on precompression and wave amplitude.

### 1.3.2. Dissipation and viscoelasticity

Soft matter is rarely purely Hamiltonian. Viscosity, friction, internal relaxation, substrate drag, and coupling to a surrounding fluid can all dissipate energy. A simple way to see the consequences is to add two common damping mechanisms to the scalar elastic wave equation:

$$\rho \partial_t^2 u = K \nabla^2 u + \eta \partial_t \nabla^2 u - \gamma \partial_t u. \tag{1.3.3}$$

The term $-\gamma \partial_t u$ describes environmental or substrate drag. It damps uniform motion and remains finite as the wavelength goes to infinity. The term $\eta \partial_t \nabla^2 u$ describes internal viscosity, or Kelvin–Voigt damping. It damps strain rates rather than uniform translation, and therefore vanishes for long-wavelength modes as $k^2$.

For a plane wave $u \sim e^{i(k\cdot r - \omega t)}$, the equation gives

$$\rho \omega^2 + i(\gamma + \eta k^2)\omega - K k^2 = 0. \tag{1.3.4}$$

Writing $c = \sqrt{K/\rho}$, the two roots are

$$\omega_\pm(k) = -\frac{i}{2\rho}\left(\gamma + \eta k^2\right) \pm \sqrt{c^2 k^2 - \left[\frac{\gamma + \eta k^2}{2\rho}\right]^2}. \tag{1.3.5}$$

Thus each Fourier mode behaves like a damped harmonic oscillator. The elastic oscillation frequency is $ck$, while the damping rate is $(\gamma + \eta k^2)/(2\rho)$.

The mode is underdamped when

$$\frac{\gamma + \eta k^2}{2\rho} < ck. \tag{1.3.6}$$

In this regime the square root is real. The mode propagates with oscillation frequency

$$\operatorname{Re}\omega_\pm = \pm\sqrt{c^2 k^2 - \left[\frac{\gamma + \eta k^2}{2\rho}\right]^2}, \tag{1.3.7}$$

and decays according to

$$\operatorname{Im}\omega_\pm = -\frac{\gamma + \eta k^2}{2\rho}. \tag{1.3.8}$$

The critical wave numbers from Eq. (1.3.6) are

$$k_\pm = \frac{\rho c \pm \sqrt{\rho^2 c^2 - \eta\gamma}}{\eta} = \frac{\sqrt{\rho K} \pm \sqrt{\rho K - \eta\gamma}}{\eta}. \tag{1.3.9}$$

If

$$\eta\gamma < \rho K, \tag{1.3.10}$$

there are two critical wave numbers. The modes are overdamped for

$$0 < k < k_- \qquad \text{or} \qquad k > k_+, \tag{1.3.11}$$

and underdamped in the intermediate window

$$k_- < k < k_+. \tag{1.3.12}$$

Thus the propagating waves live only in a finite band of wave numbers.

If

$$\eta\gamma = \rho K, \tag{1.3.13}$$

the two critical wave numbers merge at

$$k_* = \frac{\rho c}{\eta} = \frac{\sqrt{\rho K}}{\eta}. \tag{1.3.14}$$

There is no finite underdamped window: all modes are overdamped except the single critically damped mode at $k = k_*$. If

$$\eta\gamma > \rho K, \tag{1.3.15}$$

there is no real solution to the critical damping condition, and all modes are overdamped.

The two limiting cases make the physics especially clear. If $\eta = 0$, the overdamped condition becomes

$$\gamma > 2\rho c k, \tag{1.3.16}$$

so the overdamped modes are

$$0 < k < \frac{\gamma}{2\rho c}. \tag{1.3.17}$$

Pure substrate drag therefore overdamps long wavelengths first. If $\gamma = 0$, the overdamped condition becomes

$$\eta k^2 > 2\rho c k, \tag{1.3.18}$$

so, for $k > 0$,

$$k > \frac{2\rho c}{\eta}. \tag{1.3.19}$$

Pure Kelvin–Voigt damping therefore overdamps short wavelengths first. In a continuum theory, this large-$k$ statement should be interpreted below the microscopic cutoff.

This distinction is often the most important lesson. Substrate drag gives a damping rate that is nearly independent of $k$, so it dominates over the elastic frequency $ck$ at small $k$. Internal viscosity gives a damping rate proportional to $k^2$, so it dominates over $ck$ at large $k$. Therefore substrate drag kills long-wavelength sound first, while Kelvin–Voigt viscosity kills short-wavelength sound first.

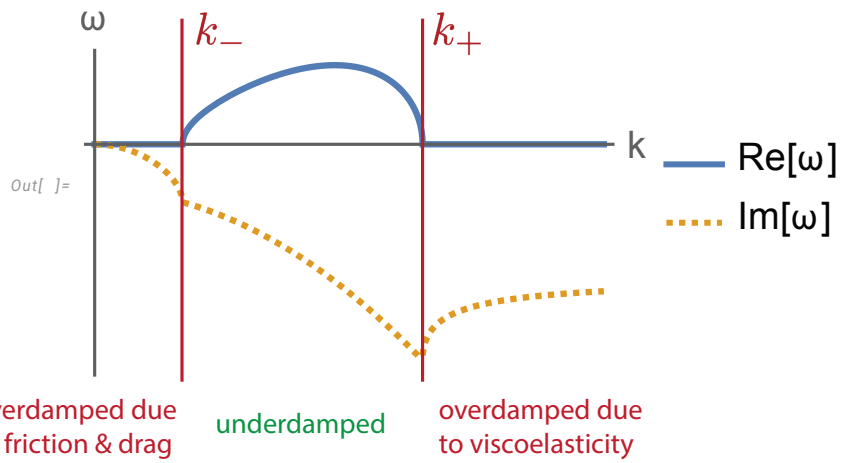


Figure 2: Wave propagation $\omega'$ and dissipation $\omega''$ as functions of wave vector $k$, in media with two types of damping: friction and viscoelasticity.

### 1.3.3. Disorder and heterogeneity

Real materials are not perfectly homogeneous. Density, stiffness, damping, and geometry may vary in space:

$$\rho \to \rho(\boldsymbol{r}), \qquad K \to K(\boldsymbol{r}). \tag{1.3.20}$$

A scalar wave equation then becomes

$$\rho(\boldsymbol{r})\partial_t^2 u = \nabla \cdot [K(\boldsymbol{r})\nabla u]\,. \tag{1.3.21}$$

Spatial heterogeneity causes scattering, attenuation, localization, effective-medium behavior, sample-to-sample variation, and breakdown of simple periodic descriptions.

Disorder is not always merely a nuisance. In structured media, disorder can couple strongly to soft modes, change transport properties, and in some systems even produce robust or anomalous boundary responses.

### 1.3.4. Internal resonances

Another way real materials go beyond the ideal wave equation is through internal degrees of freedom. Instead of a single displacement field, the material may contain local modes that can oscillate—with inertia which causes an intrinsic frequency—relative to the background continuum. This mechanism is central in acoustic and elastic metamaterials, but it does not intrinsically require a periodic structure. Periodicity is one way to arrange many resonators; the local-resonance mechanism itself is the hybridization between a propagating field and an internal oscillator.

A useful microscopic starting point is a one-dimensional mass-in-mass chain (Fig. 3). Let $u_n(t)$ be the displacement of the main mass in cell $n$, and let $v_n(t)$ be the displacement of an internal resonator attached to it. Neighboring main masses are connected by springs of stiffness $k$, and each internal resonator is connected to the corresponding main mass by a spring of stiffness $\kappa_0$:

$$M\ddot{u}_n = k(u_{n+1} + u_{n-1} - 2u_n) - \kappa_0(u_n - v_n), \tag{1.3.22}$$

$$m_r\ddot{v}_n = -\kappa_0(v_n - u_n). \tag{1.3.23}$$

The first equation says that the backbone displacement feels both the usual elastic force from neighboring cells and the force from the attached resonator. The second equation says that the internal mass is driven only by its relative displacement from the backbone.

Now take the long-wavelength limit. Let $x = na$, where $a$ is the spacing of the chain, and write

$$u_n(t) \to u(x,t), \qquad v_n(t) \to v(x,t). \tag{1.3.24}$$

For wavelengths much longer than $a$,

$$u_{n+1} + u_{n-1} - 2u_n = a^2 \partial_x^2 u + O(a^4). \tag{1.3.25}$$

Dividing Eqs. (1.3.22) and (1.3.23) by the cell size and defining the continuum parameters

$$\rho = \frac{M}{a}, \qquad m = \frac{m_r}{a}, \qquad K = ka, \qquad \kappa = \frac{\kappa_0}{a}, \tag{1.3.26}$$

we obtain the coupled continuum equations

$$\rho\, \partial_t^2 u = K \partial_x^2 u - \kappa(u - v), \tag{1.3.27}$$

$$m\, \partial_t^2 v = -\kappa(v - u). \tag{1.3.28}$$

Here $u(x,t)$ is the displacement of the main elastic continuum, while $v(x,t)$ is the displacement of the internal resonator field. The resonator has a natural frequency

$$\Omega_0 = \sqrt{\kappa/m}. \tag{1.3.29}$$

This derivation also makes clear why the model belongs naturally in a continuum-wave lecture: after homogenization, the resonator density is uniform, and no Brillouin zone is needed to understand the basic local-resonance gap.

For a uniform effective medium, take

$$u = U \mathrm{e}^{\mathrm{i}(qx - \omega t)}, \qquad v = V \mathrm{e}^{\mathrm{i}(qx - \omega t)}. \tag{1.3.30}$$

Then

$$\begin{pmatrix} Kq^2 + \kappa - \rho\omega^2 & -\kappa \\ -\kappa & \kappa - m\omega^2 \end{pmatrix} \begin{pmatrix} U \\ V \end{pmatrix} = 0. \tag{1.3.31}$$

The dispersion is determined by

$$(Kq^2 + \kappa - \rho\omega^2)(\kappa - m\omega^2) - \kappa^2 = 0. \tag{1.3.32}$$

This equation has two branches. One is acoustic-like at small $q$, and the other is resonator-like near $\Omega_0$. Near resonance, the propagating wave and the internal oscillator hybridize strongly.

Thus the two branches are

$$\omega_\pm^2(q) = \frac{mKq^2 + \kappa(m+\rho) \pm \sqrt{\left[mKq^2 + \kappa(m+\rho)\right]^2 - 4\rho m \kappa K q^2}}{2\rho m}. \tag{1.3.33}$$

It is useful to define

$$c^2 = \frac{K}{\rho}, \qquad \Omega_0^2 = \frac{\kappa}{m}, \qquad \Omega_*^2 = \kappa\left(\frac{1}{m} + \frac{1}{\rho}\right). \tag{1.3.34}$$

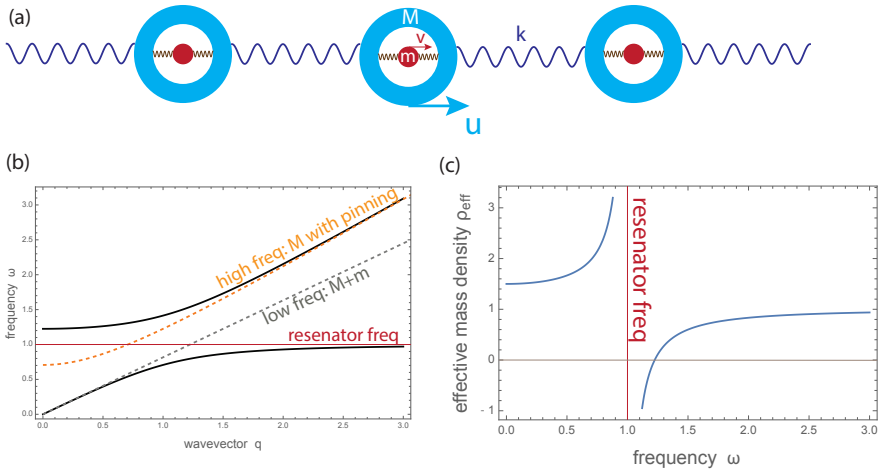


Figure 3: Mechanical system with internal resonance. (a) A mass-in-mass chain as a simple illustration of internal resonance. (b) Dispersion relation and gap due to internal resonance. (c) Frequency-dependent effective mass, with negative values near resonance.

Then the two branches can be written more transparently as

$$\omega_{\pm}^2(q) = \frac{1}{2}\left[c^2q^2 + \Omega_*^2 \pm \sqrt{\left(c^2q^2+\Omega_*^2\right)^2 - 4c^2\Omega_0^2q^2}\right]. \tag{1.3.35}$$

At small wavevector, the lower branch is acoustic:

$$\omega_-^2(q) \simeq \frac{K}{\rho+m}q^2, \qquad \omega_-(q) \simeq \sqrt{\frac{K}{\rho+m}}\,q. \tag{1.3.36}$$

The resonator moves together with the continuum, so the effective inertia is $\rho + m$.

The upper branch has a finite frequency at $q = 0$:

$$\omega_+(0) = \Omega_* = \sqrt{\kappa\left(\frac{1}{m}+\frac{1}{\rho}\right)}. \tag{1.3.37}$$

This is the out-of-phase internal mode of the continuum and the resonator.

At large wavevector, the lower branch approaches the bare resonator frequency:

$$\omega_-^2(q) \to \Omega_0^2 = \frac{\kappa}{m}, \qquad \omega_-(q) \to \Omega_0. \tag{1.3.38}$$

Thus the lower branch changes from acoustic-like at small $q$ to resonator-like at large $q$.

The upper branch becomes continuum-like at large wavevector:

$$\omega_+^2(q) \simeq c^2q^2 + \frac{\kappa}{\rho}, \qquad \omega_+(q) \simeq cq. \tag{1.3.39}$$

Thus the upper branch changes from an internal resonator mode at small $q$ to a propagating continuum wave at large $q$.

We can also eliminate $v$ to obtain a frequency-dependent effective density. From Eq. (1.3.28),

$$V = \frac{\kappa}{\kappa - m\omega^2}U = \frac{\Omega_0^2}{\Omega_0^2-\omega^2}U. \tag{1.3.40}$$

Substituting into Eq. (1.3.27) gives

$$Kq^2 = \omega^2 \rho_{\text{eff}}(\omega), \tag{1.3.41}$$

with

$$\rho_{\text{eff}}(\omega) = \rho + \frac{m\Omega_0^2}{\Omega_0^2 - \omega^2}. \tag{1.3.42}$$

Just above the local resonance, the effective density can become negative. In that frequency range, real propagating solutions are forbidden in the effective continuum model. This gives a local-resonance gap.

If the resonators themselves are arranged periodically and one studies wavelengths comparable to the resonator spacing, then Bloch's theorem can also be applied to the coupled fields:

$$\begin{pmatrix} u_q(x) \\ v_q(x) \end{pmatrix} = \mathrm{e}^{\mathrm{i}qx} \begin{pmatrix} \tilde{u}_q(x) \\ \tilde{v}_q(x) \end{pmatrix}, \qquad \begin{pmatrix} \tilde{u}_q(x+a) \\ \tilde{v}_q(x+a) \end{pmatrix} = \begin{pmatrix} \tilde{u}_q(x) \\ \tilde{v}_q(x) \end{pmatrix}. \tag{1.3.43}$$

The band structure of such a resonant metamaterial can contain both local-resonance-type gaps and Bragg-type gaps.

## 1.4. Periodic media: Bragg gaps and Bloch waves

Earlier in this lecture, the internal-resonance subsection described a *local-resonance* route to a band gap: an internal oscillator hybridizes with a propagating continuum wave. There is another, more geometric route to a band gap. It comes from spatial periodicity. The essential physics is Bragg backscattering: at special wavelengths, a wave and its reflected partner become degenerate, and a weak periodic modulation can split them into two standing waves with different elastic energies.

This section introduces that idea before introducing Bloch's theorem. This order is useful pedagogically: first understand why a gap opens, then introduce the symmetry language that organizes all bands.

### 1.4.1. Origin of a Bragg band gap

Consider a one-dimensional continuum elastic wave in a weakly periodic stiffness profile,

$$\rho_0 \partial_t^2 u = \partial_x \left[ K(x) \partial_x u \right], \qquad K(x) = K_0 + 2\delta K \cos(Gx), \qquad G = \frac{2\pi}{a}, \tag{1.4.1}$$

where $a$ is the period and $|\delta K| \ll K_0$. If $\delta K = 0$, the normal modes are ordinary plane waves with

$$\omega = c|q|, \qquad c = \sqrt{K_0/\rho_0}. \tag{1.4.2}$$

The periodic modulation can scatter a wave with wavevector $q$ into a wave with wavevector $q - G$. This scattering becomes resonant when the scattered wave is the counter-propagating partner of the original wave (4):

$$q - G = -q. \tag{1.4.3}$$

Thus

$$q = \frac{G}{2} = \frac{\pi}{a}, \qquad \lambda = \frac{2\pi}{q} = 2a. \tag{1.4.4}$$

At this wavelength, reflections from successive periods add coherently. A right-moving wave and a left-moving wave are no longer independent traveling waves; they combine into standing waves.

At the zone edge, the two real standing-wave patterns can be chosen as

$$u_c(x) = \cos\frac{Gx}{2}, \qquad u_s(x) = \sin\frac{Gx}{2}. \tag{1.4.5}$$

They have the same wavelength, but their strain fields are shifted relative to the stiffness pattern:

$$|\partial_x u_c|^2 \propto \sin^2\frac{Gx}{2} = \frac{1-\cos Gx}{2}, \qquad |\partial_x u_s|^2 \propto \cos^2\frac{Gx}{2} = \frac{1+\cos Gx}{2}. \tag{1.4.6}$$

The elastic energy is controlled by

$$E_{\text{elastic}} \sim \frac{1}{2}\int K(x)|\partial_x u|^2\,\mathrm{d}x. \tag{1.4.7}$$

Therefore one standing wave puts more strain in the stiff part of the unit cell, while the other puts more strain in the soft part. Their frequencies split. To leading order in $\delta K$,

$$\omega_c^2 \simeq \frac{G^2}{4\rho_0}(K_0 - \delta K), \qquad \omega_s^2 \simeq \frac{G^2}{4\rho_0}(K_0 + \delta K), \tag{1.4.8}$$

for the choice $K(x) = K_0 + 2\delta K\cos Gx$ with real $\delta K$. The sign assignment simply records which standing wave places its strain in the stiff region.

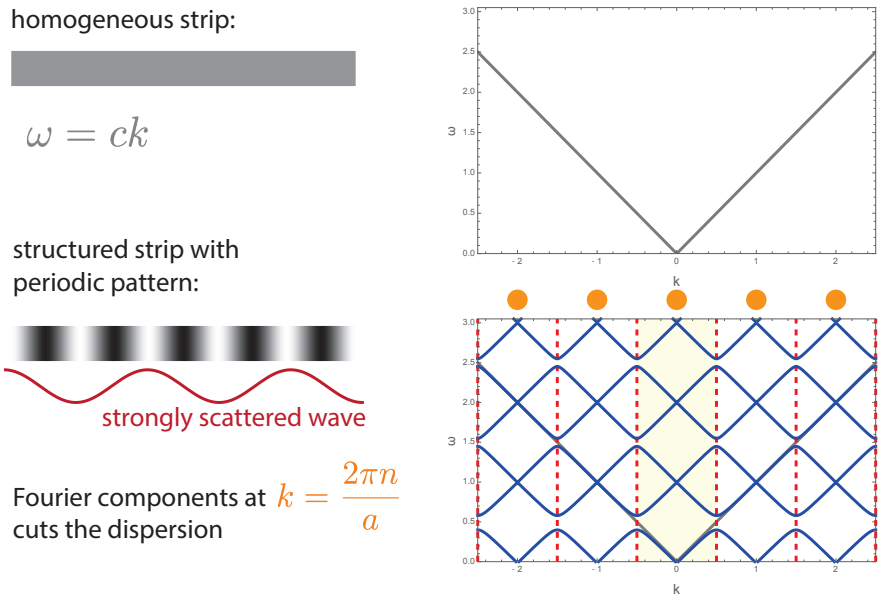


Figure 4: Waves in periodic media. Wave length $\lambda = 2a$ is the resonant condition for strong scattering, also known as the Bragg condition. This opens bandgaps at Bragg planes.

### 1.4.2. Bloch's theorem for continuum elastic waves

The band-gap argument above used only two waves near one resonance. To describe all modes in a periodic continuum, we need Bloch's theorem, which builds on the symmetry structure. Let

$$\rho(x)\partial_t^2 u = \partial_x\left[K(x)\partial_x u\right], \qquad K(x+a) = K(x), \qquad \rho(x+a) = \rho(x). \tag{1.4.9}$$

For a time-harmonic mode $u(x,t) = \psi(x)\mathrm{e}^{-\mathrm{i}\omega t}$,

$$\mathcal{L}\psi = \omega^2\rho(x)\psi, \qquad \mathcal{L}\psi \equiv -\partial_x\left[K(x)\partial_x\psi\right]. \tag{1.4.10}$$

This is a generalized eigenvalue problem for a continuum field.

Define the translation operator $\mathcal{T}_a$ by

$$(\mathcal{T}_a\psi)(x) = \psi(x+a). \tag{1.4.11}$$

Because the material coefficients are periodic, translating the field by one unit cell does not change the wave operator. Thus $\mathcal{L}$ and $\mathcal{T}_a$ commute. A normal mode can therefore be chosen to be an eigenfunction of translation:

$$\psi(x+a) = \lambda\psi(x). \tag{1.4.12}$$

For an extended mode in a lossless infinite medium, $|\lambda| = 1$, so

$$\lambda = \mathrm{e}^{\mathrm{i}qa}. \tag{1.4.13}$$

Hence

$$\psi_q(x+a) = \mathrm{e}^{\mathrm{i}qa}\psi_q(x). \tag{1.4.14}$$

Equivalently,

$$\boxed{\psi_q(x) = \mathrm{e}^{\mathrm{i}qx}v_q(x), \qquad v_q(x+a) = v_q(x).} \tag{1.4.15}$$

This is Bloch's theorem for the continuum elastic wave equation. The factor $\mathrm{e}^{\mathrm{i}qx}$ carries the phase advance from cell to cell, while $v_q(x)$ describes the periodic wave pattern inside the unit cell.

In higher-dimensional elasticity, the same statement applies to the vector displacement field. For

$$\rho(\boldsymbol{r})\partial_t^2 u_i = \partial_j\left[C_{ijkl}(\boldsymbol{r})\partial_l u_k\right], \tag{1.4.16}$$

with periodic $\rho(\boldsymbol{r})$ and $C_{ijkl}(\boldsymbol{r})$, the Bloch form is

$$u_{i,n\boldsymbol{q}}(\boldsymbol{r}) = \mathrm{e}^{\mathrm{i}\boldsymbol{q}\cdot\boldsymbol{r}}v_{i,n\boldsymbol{q}}(\boldsymbol{r}), \qquad v_{i,n\boldsymbol{q}}(\boldsymbol{r}+\boldsymbol{R}) = v_{i,n\boldsymbol{q}}(\boldsymbol{r}), \tag{1.4.17}$$

where $n$ is a band index and $\boldsymbol{R}$ is a lattice vector.

### 1.4.3. Reciprocal lattice and the first Brillouin zone

For a one-dimensional period $a$, the reciprocal lattice vectors are

$$G_m = \frac{2\pi m}{a}, \qquad m \in \mathbb{Z}. \tag{1.4.18}$$

The Bloch label $q$ is only defined modulo $G_m$, because $\mathrm{e}^{\mathrm{i}G_m x}$ is itself periodic with period $a$ and can be absorbed into $v_q(x)$. Thus

$$q \sim q + G_m. \tag{1.4.19}$$

A convenient choice of representatives is the first Brillouin zone,

$$-\frac{\pi}{a} < q \le \frac{\pi}{a}. \tag{1.4.20}$$

In higher dimensions, reciprocal lattice vectors $\boldsymbol{G}$ are defined by

$$\mathrm{e}^{\mathrm{i}\boldsymbol{G}\cdot\boldsymbol{R}} = 1 \tag{1.4.21}$$

for all lattice vectors $\boldsymbol{R}$. The first Brillouin zone is the Wigner–Seitz cell of the reciprocal lattice.

This notation also clarifies band folding (Fig. 4). Since $v_q(x)$ is periodic, it can be expanded in reciprocal-lattice harmonics:

$$v_q(x) = \sum_G u_G(q) \mathrm{e}^{\mathrm{i}Gx}. \tag{1.4.22}$$

Thus

$$\psi_q(x) = \sum_G u_G(q) \mathrm{e}^{\mathrm{i}(q+G)x}. \tag{1.4.23}$$

A Bloch wave is a coherent superposition of plane waves whose wavevectors differ by reciprocal lattice vectors. In a homogeneous medium these components would be independent. In a periodic medium, the material modulation couples them. Lecture 2 begins from this expansion and turns it into the central equation for continuum elastic bands.

**Takeaway.** The first Brillouin zone is a bookkeeping domain for wavevectors modulo reciprocal lattice vectors. The physical wave still contains many plane-wave components $q + G$, and the coupling among those components is what produces band structure.

## Take-home messages

1. **The Wave Equation as an Effective Theory:** The standard wave equation is not a fundamental microscopic law, but an emergent, long-wavelength effective field theory strongly constrained by conservation laws and symmetries. While the mathematical structure remains the same, the physical fields and underlying restoring forces span wildly across scales—from atomic displacements to entropic polymer mechanics and structural metamaterial linkages.
2. **The Breakdown of Ideality:** Real soft and structured materials routinely violate the baseline assumptions of ideal wave theory: linearity, locality, homogeneity, conservation, and reciprocity. Phenomena like viscoelastic dissipation, disorder, nonlocality, internal resosnance and thermal fluctuations are not minor details frequently dominate the system and alter wave propagation into structural relaxation or localization.
3. **Three mechanisms for gaps:** We discussed three types of mechanisms in mechanics that gives rise to gaps in elastic waves.
   (a) pinning gap: at $\omega = 0$, width $\omega_0$
   (b) local-resonance gap: at $\omega = \Omega_0$, width controlled by coupling
   (c) Bragg gap: at $\omega = \omega(G/2)$, width $|U_G|$

   They come from very different origins but share the same phenomena of blocking waves from propagation in a media.
4. **Periodicity and Bragg Band Gaps:** Spatial periodicity fundamentally reorganizes wave propagation through coherent backscattering. At high symmetry points where forward- and backward-traveling waves become degenerate, a periodic modulation splits the modes into standing waves with distinct energies, generating a forbidden Bragg band gap.
5. **Bloch's Theorem and Reciprocal Space:** In a periodic medium, homogeneous plane waves are no longer independent; they are strongly coupled by the material's Fourier components. Bloch's theorem provides the native geometric language for these waves, framing them as a coherent superposition of plane waves wrapped cleanly into a finite bookkeeping domain: the first Brillouin zone (BZ).

## Further reading


1. P. M. Chaikin and T. C. Lubensky, *Principles of Condensed Matter Physics*, Cambridge University Press (1995). See especially the chapters on elasticity, hydrodynamics, and soft condensed matter.
2. M. Doi, *Soft Matter Physics*, Oxford University Press (2013). A concise introduction to entropic elasticity, interfaces, polymers, gels, and viscoelastic response.
3. C. Kittel, *Introduction to Solid State Physics*, 8th ed., Wiley (2005). See the discussion of lattice vibrations, reciprocal space, Brillouin zones, and the nearly-free-electron central equation.
4. N. W. Ashcroft and N. D. Mermin, *Solid State Physics*, Holt, Rinehart and Winston (1976). A standard reference for Bloch's theorem, reciprocal lattices, Brillouin zones, and band formation in periodic media.

## Homework 1: Symmetry, Lagrangians, and Bloch Waves

A central theme of Lecture 1 is that the wave equation is an effective long-wavelength theory. Its ideal form is strongly constrained by symmetry, while real soft and structured materials often contain damping mechanisms that change wave propagation into relaxation.

Consider a scalar displacement-like field $u(x,t)$ in one spatial dimension.

### Part A: Wave equation from a Lagrangian

Consider the leading-order Lagrangian density of an elastic medium

$$\mathcal{L} = \frac{\rho}{2}(\partial_t u)^2 - \frac{K}{2}(\partial_x u)^2. \tag{1.4.24}$$

(1) Explain the physical meaning of the two terms in $\mathcal{L}$. Discuss what symmetries have been used to eliminate other leading order terms.

(2) What symmetry do you need to break to allow a term proportional to $u^2$? What about a term proportional to $\partial_x u$?

(3) Use the Euler–Lagrange equation for fields,

$$\frac{\partial \mathcal{L}}{\partial u} - \partial_t \frac{\partial \mathcal{L}}{\partial(\partial_t u)} - \partial_x \frac{\partial \mathcal{L}}{\partial(\partial_x u)} = 0, \tag{1.4.25}$$

to derive

$$\rho \partial_t^2 u = K \partial_x^2 u. \tag{1.4.26}$$

(4) Identify the wave speed $c$.

(5) Suppose a term

$$-\frac{\kappa}{2}u^2 \tag{1.4.27}$$

is added to the Lagrangian density. Derive the modified equation of motion and the dispersion relation. What physical kind of mode does this describe?

### Part B: What do Bloch waves look like?

Lecture 1 introduced Bloch's theorem for waves in periodic media. The goal of this homework is to understand what a Bloch wave looks like in real space, how it translates from one unit cell to the next, and why the Bloch wavevector is only defined modulo a reciprocal lattice vector.

Consider a one-dimensional periodic medium with lattice constant $a$:

$$\rho(x)\partial_t^2 u = \partial_x \left[K(x)\partial_x u\right], \qquad K(x+a) = K(x), \qquad \rho(x+a) = \rho(x). \tag{1.4.28}$$

For a time-harmonic mode $u(x,t) = \psi(x)e^{-i\omega t}$, Bloch's theorem says

$$\psi_q(x) = e^{iqx} v_q(x), \qquad v_q(x+a) = v_q(x). \tag{1.4.29}$$

1. Show that a Bloch wave satisfies

$$\psi_q(x+a) = e^{iqa}\psi_q(x). \tag{1.4.30}$$

Explain in words why a Bloch wave is not necessarily periodic with period $a$, even though the medium is periodic with period $a$.

2. Show that $q$ and $q+G$ describe the same Bloch sector. More explicitly, show that

$$\psi_q(x) = e^{iqx} v_q(x) \tag{1.4.31}$$

can also be written in the form

$$\psi_q(x) = e^{i(q+G)x} v_{q+G}(x), \tag{1.4.32}$$

where $v_{q+G}(x)$ is still periodic with period $a$. What is $v_{q+G}(x)$ in terms of $v_q(x)$?

**Optional visualization.** Take

$$v_q(x) = 1 + \epsilon \cos(Gx), \qquad G = \frac{2\pi}{a}. \tag{1.4.33}$$

Sketch or plot the real part of

$$\psi_q(x) = e^{iqx} v_q(x) \tag{1.4.34}$$

over several unit cells for

$$q = 0, \qquad q = \frac{\pi}{2a}, \qquad q = \frac{\pi}{a}. \tag{1.4.35}$$

# Lecture 2: Band Structures and Geometry of Mechanical Waves

**Overview.** Building on the symmetry foundations and plane-wave descriptions established in Lecture 1, this lecture lays out the fundamental framework of computing band structures, as well as formulating a deep analogy between differential geometry and wave geometry, building essential tools for discussing topological states. We begin by deriving the continuum elastic version of the central equation, demonstrating how periodic density and stiffness modulations couple discrete plane-wave components across the reciprocal lattice. We then analyze the two-wave approximation near a Bragg plane to solve for the explicit opening of a zone-edge band gap under a weak periodic modulation. After surveying the universal appearance of this band structure framework across diverse physical platforms, we transition to the underlying geometry of the wave eigenvectors. Finally, we establish the mathematical language of vector bundles, framing wave-function geometry via a real-space analogy, mapping out the Berry connection, Zak phase, and their higher-dimensional extensions to 2D Berry curvature and Chern numbers, and defining the quantum metric as a gauge-invariant measure of distance between neighboring wave patterns.

## 2.1. The central equation for continuum elastic waves

### 2.1.1. Deriving the central equation

We now derive the elastic analogue of the central equation for electron bands. The useful bookkeeping is to expand the wave in ordinary plane waves first, and only afterward use periodicity to see which plane waves are coupled.

Start from the scalar continuum equation introduced in Lecture 1,

$$\rho(x)\partial_t^2 u = \partial_x \left[K(x)\partial_x u\right], \qquad K(x+a) = K(x), \qquad \rho(x+a) = \rho(x). \tag{2.1.1}$$

For a time-harmonic mode $u(x,t) = \psi(x)\mathrm{e}^{-\mathrm{i}\omega t}$, this becomes

$$\partial_x \left[K(x)\partial_x \psi(x)\right] + \omega^2 \rho(x)\psi(x) = 0. \tag{2.1.2}$$

The periodic coefficients have Fourier expansions

$$K(x) = \sum_G K_G \mathrm{e}^{\mathrm{i}Gx}, \qquad \rho(x) = \sum_G \rho_G \mathrm{e}^{\mathrm{i}Gx}, \qquad G = \frac{2\pi m}{a}. \tag{2.1.3}$$

Here $G$ is a reciprocal-lattice vector. The average values are $K_0$ and $\rho_0$.

Now expand the wave itself in plane waves,

$$\psi(x) = \sum_k C_k \mathrm{e}^{\mathrm{i}kx}, \qquad k = \frac{2\pi n}{L}, \tag{2.1.4}$$

where $L$ is the large system size. At this stage $k$ is simply an allowed plane-wave wavevector. We have not yet chosen a first-zone Bloch label.

Substituting Eqs. (2.1.3) and (2.1.4) into Eq. (2.1.2), the mass term gives

$$\rho(x)\psi(x) = \sum_k \left( \sum_G \rho_G C_{k-G} \right) \mathrm{e}^{\mathrm{i}kx}. \tag{2.1.5}$$

The elastic term gives

$$\partial_x \left[K(x)\partial_x \psi(x)\right] = -\sum_k \left(\sum_G k(k-G)K_G C_{k-G}\right) \mathrm{e}^{\mathrm{i}kx}. \tag{2.1.6}$$

Equating the coefficient of each plane wave $\mathrm{e}^{\mathrm{i}kx}$ gives

$$\boxed{\sum_G \left[k(k-G)K_G - \omega^2 \rho_G\right] C_{k-G} = 0} \tag{2.1.7}$$

for every allowed wavevector $k$. This is the central equation for the scalar continuum elastic problem. It is the direct analogue of Kittel's central equation, except that the eigenvalue is $\omega^2$, and the periodic elastic medium can place Fourier components in both the stiffness and the density.

It is often useful to separate the average medium from the modulation:

$$\left(K_0 k^2 - \rho_0 \omega^2\right) C_k + \sum_{G\neq 0} \left[k(k-G)K_G - \omega^2 \rho_G\right] C_{k-G} = 0. \tag{2.1.8}$$

For constant density, this reduces to the especially transparent form

$$\left(K_0 k^2 - \rho_0 \omega^2\right) C_k + \sum_{G\neq 0} k(k-G)K_G C_{k-G} = 0. \tag{2.1.9}$$

The first term is the homogeneous elastic dispersion. The remaining terms say that a stiffness modulation with wavevector $G$ scatters a plane wave $k-G$ into the plane wave $k$.

This form also makes Bloch's theorem almost automatic. If one coefficient $C_k$ appears in a solution, Eq. (2.1.7) only connects it to coefficients whose wavevectors differ from $k$ by reciprocal-lattice vectors. Therefore one closed block of the problem has the form

$$\psi_q(x) = \sum_G C_{q+G} \mathrm{e}^{\mathrm{i}(q+G)x}, \qquad q \in \text{first Brillouin zone}. \tag{2.1.10}$$

Equivalently,

$$\psi_q(x) = \mathrm{e}^{\mathrm{i}qx} u_q(x), \qquad u_q(x) = \sum_G C_{q+G} \mathrm{e}^{\mathrm{i}Gx}, \qquad u_q(x+a) = u_q(x). \tag{2.1.11}$$

Thus the central equation is not separate from Bloch's theorem. It is the plane-wave form of the wave equation after translation symmetry has block-diagonalized the problem into independent Bloch sectors.

For later use, it is helpful to rewrite the same equation as a matrix problem within one fixed Bloch sector. Define $c_G(q) = C_{q+G}$. Then Eq. (2.1.7) becomes

$$\sum_{G'} (q+G)(q+G') K_{G-G'} c_{G'}(q) = \omega^2 \sum_{G'} \rho_{G-G'} c_{G'}(q). \tag{2.1.12}$$

This is the $q$-block of the central equation. It is the form one actually diagonalizes to obtain elastic bands.

**Takeaway.** The central equation is a set of equations for the plane-wave coefficients $C_k$. Periodicity only couples $k$ to $k-G$. Choosing one equivalence class $k = q+G$ gives the Bloch eigenvalue problem at fixed crystal momentum $q$.

The same structure holds for vector elasticity. For

$$\rho(\boldsymbol{r})\partial_t^2 u_i = \partial_j \left[C_{ijkl}(\boldsymbol{r})\partial_l u_k\right], \tag{2.1.13}$$

with Bloch expansion $u_i(\boldsymbol{r}) = \sum_{\boldsymbol{G}} u_{i,\boldsymbol{G}} \mathrm{e}^{\mathrm{i}(\boldsymbol{q}+\boldsymbol{G})\cdot\boldsymbol{r}}$, the central equation becomes

$$\sum_{\boldsymbol{G}',j,k,l} (q_j + G_j) C_{ijkl,\boldsymbol{G}-\boldsymbol{G}'} (q_l + G'_l) u_{k,\boldsymbol{G}'} = \omega^2 \sum_{\boldsymbol{G}'} \rho_{\boldsymbol{G}-\boldsymbol{G}'} u_{i,\boldsymbol{G}'}. \tag{2.1.14}$$

The scalar model is therefore not a different kind of physics; it is the cleanest way to see the reciprocal-space structure before adding polarization indices.

### 2.1.2. Two-wave solution near a Bragg plane

Now specialize to constant density and a weak first harmonic in the stiffness,

$$K(x) = K_0 + K_G \mathrm{e}^{\mathrm{i}Gx} + K_{-G} \mathrm{e}^{-\mathrm{i}Gx}, \qquad |K_G| \ll K_0. \tag{2.1.15}$$

For a real sinusoidal modulation, $K(x)$ is real, so $K^*_{-G} = K_G \equiv \delta K = |\delta K| \mathrm{e}^{\mathrm{i}\phi}$ where the phase information represent a shift in real space.

The central equation, Eq. (2.1.9), tells us which two plane waves become strongly coupled. Near the first Bragg plane, write

$$k = \frac{G}{2} + \kappa. \tag{2.1.16}$$

The component $C_k$ is nearly degenerate with $C_{k-G}$, because

$$k_+ \equiv k = \frac{G}{2} + \kappa, \qquad k_- \equiv k - G = -\frac{G}{2} + \kappa, \tag{2.1.17}$$

obey $k_+^2 = k_-^2$ at $\kappa = 0$. Retaining only these two coefficients,

$$c_+ \equiv C_{k_+}, \qquad c_- \equiv C_{k_-}, \tag{2.1.18}$$

Eq. (2.1.9) gives

$$\rho_0 \omega^2 \begin{pmatrix} c_+ \\ c_- \end{pmatrix} = \begin{pmatrix} K_0 k_+^2 & \delta K\, k_+ k_- \\ \delta K^*\, k_+ k_- & K_0 k_-^2 \end{pmatrix} \begin{pmatrix} c_+ \\ c_- \end{pmatrix}. \tag{2.1.19}$$

This is the minimal two-band problem produced by the central equation. It is just the two-dimensional subspace spanned by the two Bragg-coupled plane waves $k$ and $k - G$.

The two squared frequencies are

$$\omega_\pm^2(\kappa) = \frac{1}{\rho_0} \left[ K_0 \left( \frac{G^2}{4} + \kappa^2 \right) \pm \sqrt{(K_0 G \kappa)^2 + |\delta K|^2 \left( \frac{G^2}{4} - \kappa^2 \right)^2} \right]. \tag{2.1.20}$$

At the Bragg plane, $\kappa = 0$, this reduces to

$$\omega_\pm^2(0) = \frac{G^2}{4\rho_0} \left( K_0 \pm |\delta K| \right). \tag{2.1.21}$$

Thus the gap in squared frequency is

$$\Delta(\omega^2) = \frac{G^2 |\delta K|}{2\rho_0}. \tag{2.1.22}$$

For weak modulation, the corresponding frequency gap near

$$\omega_B = \frac{G}{2}\sqrt{K_0/\rho_0} \tag{2.1.23}$$

is approximately

$$\Delta\omega \simeq \frac{G|\delta K|}{2\sqrt{\rho_0 K_0}}. \tag{2.1.24}$$

For real positive $\delta K$, the zone-edge eigenmodes are the two standing waves discussed in Lecture 1:

$$\mathrm{e}^{\mathrm{i}Gx/2} + \mathrm{e}^{-\mathrm{i}Gx/2} \sim \cos\frac{Gx}{2}, \qquad \mathrm{e}^{\mathrm{i}Gx/2} - \mathrm{e}^{-\mathrm{i}Gx/2} \sim \sin\frac{Gx}{2}, \tag{2.1.25}$$

up to an overall phase and a convention-dependent assignment of the $+$ and $-$ band labels. One standing wave concentrates strain in the softer part of the unit cell and has the lower frequency. The other concentrates strain in the stiffer part and has the higher frequency.

Equation (2.1.19) can also be written in Pauli-matrix form:

$$\rho_0\omega^2 \simeq K_0\left(\frac{G^2}{4}+\kappa^2\right) I + K_0 G\kappa\,\sigma_z + \left(\kappa^2 - \frac{G^2}{4}\right)\left[\mathrm{Re}\,\delta K\,\sigma_x - \mathrm{Im}\,\delta K\,\sigma_y\right]. \tag{2.1.26}$$

Very close to the Bragg plane, the term $K_0 G\kappa\,\sigma_z$ is the detuning between the two folded waves, while the term proportional to $\delta K$ opens the gap. This is why the zone-edge Bragg gap is the local prototype of a two-band avoided crossing.

### 2.1.3. Where this structure appears

The central equation is useful because the same structure appears whenever a linear wave problem has periodic coefficients. The microscopic physics changes from system to system, but the logic is the same: write the linear wave equation, expand the periodic coefficients in reciprocal lattice vectors, and obtain a Bloch eigenvalue problem at fixed $q$.

#### Elastic and acoustic waves

Periodic density or elastic moduli produce phononic bands and acoustic band gaps. In continuum elasticity the starting point is

$$\rho(\boldsymbol{r})\partial_t^2 u_i = \partial_j\big[C_{ijkl}(\boldsymbol{r})\partial_l u_k\big], \qquad C_{ijkl}(\boldsymbol{r}+\boldsymbol{R}) = C_{ijkl}(\boldsymbol{r}), \quad \rho(\boldsymbol{r}+\boldsymbol{R}) = \rho(\boldsymbol{r}). \tag{2.1.27}$$

After the Bloch expansion, this becomes the matrix version of the central equation,

$$\sum_{\boldsymbol{G}'}(q_j+G_j)C_{ijkl,\boldsymbol{G}-\boldsymbol{G}'}(q_l+G'_l)u_{k,\boldsymbol{G}'} = \omega^2\sum_{\boldsymbol{G}'}\rho_{\boldsymbol{G}-\boldsymbol{G}'}u_{i,\boldsymbol{G}'}. \tag{2.1.28}$$

Layered media, phononic crystals, porous solids, granular chains, architected lattices, and soft composites are all examples of this class.

#### Mechanical metamaterials

For a discrete mechanical lattice, the continuum operator is replaced by a stiffness or dynamical matrix. If $u_{a,\boldsymbol{R}}$ is the displacement of degree of freedom $a$ in unit cell $\boldsymbol{R}$, a typical linear equation is

$$m_a\ddot{u}_{a,\boldsymbol{R}} = -\sum_{b,\boldsymbol{R}'}\Phi_{ab}(\boldsymbol{R}-\boldsymbol{R}')u_{b,\boldsymbol{R}'}. \tag{2.1.29}$$

Using $u_{a,\boldsymbol{R}} = u_a(\boldsymbol{q})\mathrm{e}^{\mathrm{i}(\boldsymbol{q}\cdot\boldsymbol{R}-\omega t)}$ gives

$$\sum_b D_{ab}(\boldsymbol{q})u_b(\boldsymbol{q}) = \omega^2 u_a(\boldsymbol{q}), \qquad D_{ab}(\boldsymbol{q}) = \frac{1}{\sqrt{m_a m_b}}\sum_{\boldsymbol{R}} \Phi_{ab}(\boldsymbol{R})\mathrm{e}^{-\mathrm{i}\boldsymbol{q}\cdot\boldsymbol{R}}. \tag{2.1.30}$$

Periodic geometry and internal resonators therefore allow one to engineer wave speeds, band gaps, flat bands, directional propagation, and edge or interface modes. In soft matter, the relevant periodicity may come from self-assembly, swelling patterns, patterned activity, or imposed architecture.

### Photonic crystals

Maxwell's equations in a periodic dielectric medium lead to photonic bands. A common Hermitian form uses the magnetic field:

$$\nabla \times \left[\frac{1}{\epsilon(\boldsymbol{r})}\nabla \times \mathbf{H}(\boldsymbol{r})\right] = \frac{\omega^2}{c^2}\mathbf{H}(\boldsymbol{r}), \qquad \epsilon(\boldsymbol{r}+\boldsymbol{R}) = \epsilon(\boldsymbol{r}). \tag{2.1.31}$$

With

$$\mathbf{H}_{\boldsymbol{q}}(\boldsymbol{r}) = \mathrm{e}^{\mathrm{i}\boldsymbol{q}\cdot\boldsymbol{r}}\sum_{\boldsymbol{G}} \mathbf{h}_{\boldsymbol{G}}(\boldsymbol{q})\mathrm{e}^{\mathrm{i}\boldsymbol{G}\cdot\boldsymbol{r}}, \tag{2.1.32}$$

one obtains a reciprocal-space matrix problem closely analogous to the elastic central equation. The dielectric function $\epsilon(\boldsymbol{r})$ plays the role of a periodic material coefficient.

### Electrons in crystals

For electrons the starting point is the Schrödinger equation with a periodic potential,

$$\left[-\frac{\hbar^2\nabla^2}{2m} + U(\boldsymbol{r})\right]\psi(\boldsymbol{r}) = E\psi(\boldsymbol{r}), \qquad U(\boldsymbol{r}+\boldsymbol{R}) = U(\boldsymbol{r}). \tag{2.1.33}$$

Expanding $U(\boldsymbol{r}) = \sum_{\boldsymbol{G}} U_{\boldsymbol{G}}\mathrm{e}^{\mathrm{i}\boldsymbol{G}\cdot\boldsymbol{r}}$ and $\psi(\boldsymbol{r}) = \sum_{\boldsymbol{k}} C_{\boldsymbol{k}}\mathrm{e}^{\mathrm{i}\boldsymbol{k}\cdot\boldsymbol{r}}$ gives Kittel's central equation,

$$\left(\frac{\hbar^2 k^2}{2m} - E\right)C_{\boldsymbol{k}} + \sum_{\boldsymbol{G}} U_{\boldsymbol{G}}C_{\boldsymbol{k}-\boldsymbol{G}} = 0. \tag{2.1.34}$$

This is the historically familiar setting for Bloch's theorem, but the theorem itself is a general statement about waves in periodic media.

### Magnons, polaritons, plasmons, and other collective modes

Many collective modes are described by first-order-in-time or coupled-field equations rather than by the scalar elastic equation. After linearization, they still have the form

$$\mathrm{i}\partial_t\Phi(\boldsymbol{r},t) = \mathcal{L}(\boldsymbol{r},-\mathrm{i}\nabla)\Phi(\boldsymbol{r},t), \qquad \mathcal{L}(\boldsymbol{r}+\boldsymbol{R},-\mathrm{i}\nabla) = \mathcal{L}(\boldsymbol{r},-\mathrm{i}\nabla), \tag{2.1.35}$$

or, for second-order oscillator variables, an equivalent generalized eigenvalue problem. A Bloch expansion gives

$$\sum_{\boldsymbol{G}'} \mathcal{L}_{\boldsymbol{G}\boldsymbol{G}'}(\boldsymbol{q})\phi_{\boldsymbol{G}'}(\boldsymbol{q}) = \omega(\boldsymbol{q})\phi_{\boldsymbol{G}}(\boldsymbol{q}). \tag{2.1.36}$$

This covers spin waves in periodic magnets, polaritons in periodic optical media, plasmons in patterned conductors, and other linear collective excitations.

**Takeaway.** Bloch theory is a symmetry framework for waves in periodic media. Mechanical waves are one of its most direct and physically intuitive realizations, but the same reciprocal-space bookkeeping appears in many other wave problems.

## 2.2. From Bloch waves to vector bundles

The band structure $\omega_n(k)$ is only half of the story. It tells us the allowed frequencies, but not how the wave pattern changes as we move through the Brillouin zone. The eigenvector $|u_n(k)\rangle$ contains this missing information. Its components describe the relative amplitudes and phases of the internal degrees of freedom in the unit cell. The rest of this lecture focuses on the geometry of these eigenvectors.

The central equation already contains the Bloch dynamical matrix. In Eq. (2.1.12), fix a Bloch wavevector $q$ and collect the plane-wave coefficients into a vector

$$|c(q)\rangle = (\dots, c_{-G}(q), c_0(q), c_G(q), \dots)^T. \tag{2.2.1}$$

Then the central equation has the generalized eigenvalue form

$$\mathsf{K}(q)\,|c_n(q)\rangle = \omega_n^2(q)\mathsf{M}(q)\,|c_n(q)\rangle\,, \tag{2.2.2}$$

with matrix elements

$$\mathsf{K}_{GG'}(q) = (q+G)(q+G')K_{G-G'}, \qquad \mathsf{M}_{GG'}(q) = \rho_{G-G'}. \tag{2.2.3}$$

For constant density, $\mathsf{M}(q) = \rho_0 I$, so the ordinary Bloch dynamical matrix is simply

$$D(q) = \rho_0^{-1}\mathsf{K}(q). \tag{2.2.4}$$

The two-wave model in Eq. (2.1.19) is the $2\times 2$ truncation of this same $D(q)$ near a Bragg plane. Thus $D(q)$ is not a new assumption; it is the central equation restricted to one Bloch sector and represented in a chosen basis.

In the rest of this section we use the standard band-geometry notation $k$ for the Bloch wavevector. After Bloch reduction, the equation of motion can often be written as

$$D(k)\,|u_n(k)\rangle = \omega_n^2(k)\,|u_n(k)\rangle\,, \tag{2.2.5}$$

where $D(k)$ is the Bloch dynamical matrix. More generally, continuum wave problems may produce a generalized eigenvalue problem,

$$\mathsf{K}(k)\,|u_n(k)\rangle = \omega_n^2(k)\mathsf{M}(k)\,|u_n(k)\rangle\,. \tag{2.2.6}$$

If $\mathsf{M}(k)$ is positive definite, one can pass to mass-weighted variables and obtain a Hermitian eigenvalue problem of the form Eq. (2.2.5). The precise inner product matters, but the geometric idea is the same: at each $k$, the eigenvector describes the internal pattern of the wave inside one unit cell.

The discussion so far emphasized the band functions $\omega_n(k)$. Topology asks about the global structure of the eigenvectors. In one dimension, the first Brillouin zone is a circle,

$$k \in S^1. \tag{2.2.7}$$

For each momentum $k$, an isolated band gives a vector space spanned by $|u_n(k)\rangle$. Thus the band defines a vector bundle over the Brillouin zone:

$$k \mapsto \mathrm{span}\{|u_n(k)\rangle\}. \tag{2.2.8}$$

The base space is the Brillouin zone, and the fiber over each $k$ is the space of allowed wave patterns for that band. A smooth choice of normalized eigenvector $|u_n(k)\rangle$ is a local section of this bundle.

Definition: Vector bundle (intuitive/physics version)

A vector bundle is a smooth collection of vector spaces attached to the points of a base space, $\mathcal{B}$. To every point $p \in \mathcal{B}$, we attach a vector space $V_p$. The vector bundle is the collection

$$V = \{V_p \mid p \in \mathcal{B}\}. \tag{2.2.9}$$

The vector space $V_p$ is called the fiber over $p$. The fibers are required to vary smoothly as $p$ moves in $\mathcal{B}$, and they all have the same dimension. This dimension is called the rank of the vector bundle.
A **section** of the bundle is a smooth choice of one vector from each fiber:

$$v : \mathcal{B} \to V, \qquad v(p) \in V_p. \tag{2.2.10}$$

Note: This definition follows the viewpoint of A. S. Sergeev, "Topological insulators and geometry of vector bundles," SciPost Physics Lecture Notes **67** (2023), which I find helpful for the context of our discussion.

This language is useful because the eigenvector itself has a gauge freedom:

$$|u_n(k)\rangle \quad \text{and} \quad e^{\mathrm{i}\chi(k)}\,|u_n(k)\rangle \tag{2.2.11}$$

represent the same physical wave pattern. Therefore the meaningful object is not the absolute phase of the eigenvector at one $k$, but how the line $\mathrm{span}\{|u_n(k)\rangle\}$ is connected from one momentum to the next. The geometry of the bundle tells us whether these local choices can be glued together into a globally smooth and periodic choice over the whole Brillouin zone.

Equivalently, as $k$ moves, we need a rule for comparing eigenvectors that live in nearby fibers. The Berry connection is this rule of comparison. It keeps track of the phase accumulated when the wave eigenvector is parallel transported around the Brillouin zone. If the accumulated phase is nontrivial, the band has a topology of how its unit-cell vibration pattern twists in momentum space.

The question is whether this vector bundle can be smoothly deformed into a trivial one without closing the relevant band gap or breaking the symmetry that quantizes the invariant.

### 2.2.1. Wave-function geometry and the real-space geometry analogy

Since this school has already introduced differential geometry, it is useful to phrase band topology in a directly geometric language. In ordinary real-space geometry, one studies a manifold together with tangent spaces attached to each point. A vector field is a smooth choice of a vector in each tangent space. A connection tells us how to compare vectors at nearby points, and parallel transport around a closed loop can produce a nontrivial holonomy.

The geometry of waves in a periodic medium has the same structure, with the roles shifted from real space to momentum space. The base manifold is the Brillouin zone. The fiber over a point $k$ is the internal space of unit-cell wave patterns. For a single isolated band, the physically meaningful fiber is the line

$$\mathrm{span}\{|u_n(k)\rangle\}. \tag{2.2.12}$$

A smooth eigenvector $|u_n(k)\rangle$ is a choice of local section. The phase freedom

$$|u_n(k)\rangle \to e^{\mathrm{i}\chi(k)}\,|u_n(k)\rangle \tag{2.2.13}$$

is the gauge freedom of choosing a local frame in that line bundle.

Table 1: Comprehensive analogy between the differential geometry and wave geometry.

| **Geometric Concept** | **Vector Bundle** ($TM \to M$) | **Band Bundle** ($\mathcal{E} \to$ **BZ**) | **Gauge Transformation** |
|---|---|---|---|
| **Base Space & Coords** | Smooth manifold $M$ (e.g., $S^2$); Local coordinates $x^\mu$ | Brillouin Zone (BZ $\simeq T^d$); Momentum components $k_\mu$ | — |
| **Local Section (State)** | Vector field $V(x) = V^\mu(x)\frac{\partial}{\partial x^\mu}$ | Cell-periodic Bloch state $\lvert u_n(\mathbf{k})\rangle$ | $\lvert u'_n(\mathbf{k})\rangle = e^{i\theta(\mathbf{k})}\lvert u_n(\mathbf{k})\rangle$ |
| **Connection** | Connection coefficients $\Gamma^a_{b\mu}$ | Berry Connection $A^{(n)}_\mu(\mathbf{k}) = i\langle u_n(\mathbf{k})\rvert \partial_{k_\mu}\lvert u_n(\mathbf{k})\rangle$ (Gauge potential) | $\mathbf{A}'^{(n)} = \mathbf{A}^{(n)} - \nabla_{\mathbf{k}}\theta(\mathbf{k})$ |
| **Curvature** | Riemann Tensor $R^a{}_{b\mu\nu}$ | Berry Curvature $\Omega^{(n)}_{\mu\nu} = \partial_{k_\mu}A^{(n)}_\nu - \partial_{k_\nu}A^{(n)}_\mu$ (Field strength) | $\Omega'^{(n)}_{\mu\nu} = \Omega^{(n)}_{\mu\nu}$ **(Strictly Local Invariant)** |
| **Metric Tensor** | Riemannian metric $g_{\mu\nu}$ defining distances $ds^2 = g_{\mu\nu}dx^\mu dx^\nu$ | Quantum Metric $g_{\mu\nu}(\mathbf{k})$ defining state distance $ds^2 = 1 - \lvert\langle u(\mathbf{k})\rvert u(\mathbf{k}+d\mathbf{k})\rangle\rvert^2$ | $g_{\mu\nu}(\mathbf{k}) = \mathrm{Re}[\mathcal{Q}_{\mu\nu}(\mathbf{k})]$ **(Strictly Local Invariant)** |
| **1D / Loop Quantities** | Parallel transport holonomy around a loop | **Berry Phase** $\gamma_n = \oint_{\mathcal{C}} \mathbf{A}^{(n)} \cdot d\mathbf{k}$ **Zak Phase** $\gamma_{\mathrm{Zak}} = \int_{-\pi/a}^{\pi/a} A^{(n)}(k)\,dk$ | $\gamma' = \gamma - 2\pi m$ **(Invariant** (mod $2\pi$)**)** |
| **2D Global Invariant** | Euler Characteristic $\chi(M)$ via Gauss-Bonnet theorem | **First Chern Number** $C_n = \frac{1}{2\pi}\int_{\mathrm{BZ}} \Omega^{(n)}_{xy}(\mathbf{k})\,dk_x dk_y$ | $\Delta C_n = 0$ **(Strictly Global Invariant)** |
| **Physical Meaning** | Geometric holes (genus $g$): $\frac{1}{2\pi}\int_M K\,dA = 2(1-g)$ | Global "twisting" of the wavefunctions over the BZ torus | **Controls physics on the edge & interfaces: bulk-edge correspondence** |

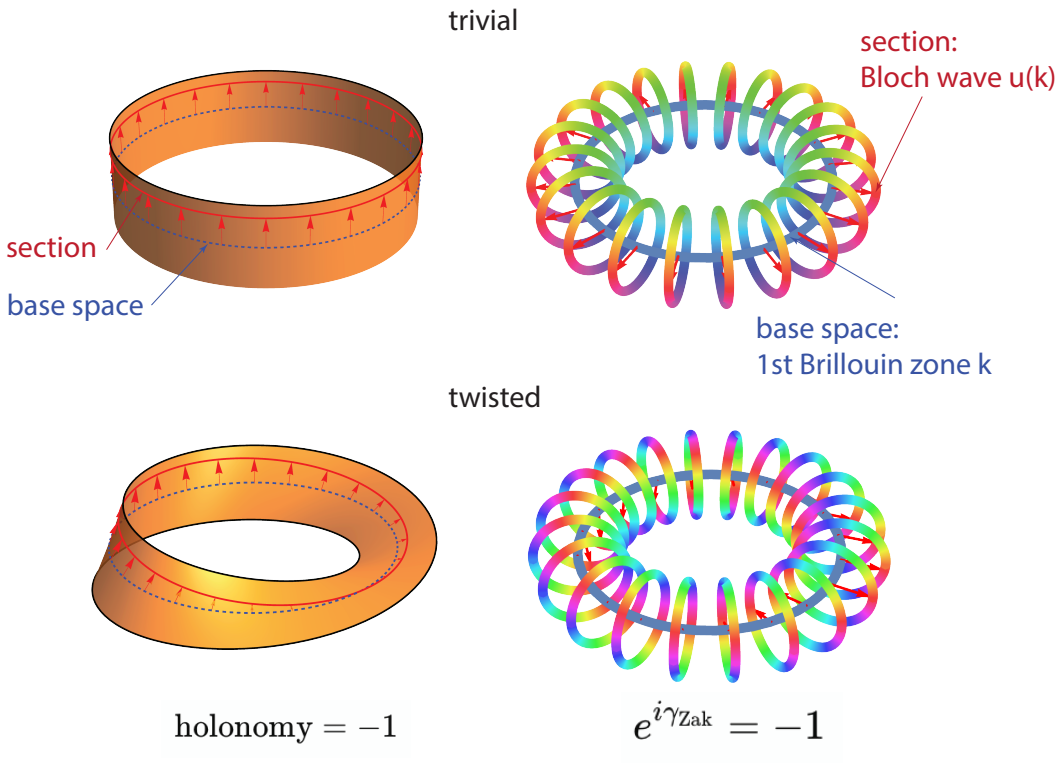


Figure 5: Analogy between vector bundles in geometry and wave geometry. The left column shows real vector bundles over a circular base space. The top panel is trivial and admits a global smooth nonzero section (red arrows). The bottom panel is Möbius-like: after one loop around the base, the fiber orientation is reversed, giving $\mathrm{Hol} = -1$, so a global nonzero smooth section is obstructed. The right column shows the analogous band-bundle picture over the one-dimensional Brillouin zone. At each momentum $k$, the fiber is the Bloch eigenspace, and choosing $u(k)$ is a gauge choice, or section (red arrows). A nontrivial Zak phase gives Berry holonomy: for $\gamma_{\mathrm{Zak}} = \pi$, parallel transport around the Brillouin zone gives $e^{i\gamma_{\mathrm{Zak}}} = -1$. Thus the Möbius twist is a real-bundle analogue of Berry-phase holonomy. *This is meant to be a schematic picture only: the real physics is more complicated: In 1D this is a holonomy effect, while in 2D a nonzero Chern number gives a true obstruction to a globally smooth periodic Bloch gauge.

This analogy is more than language. It gives a useful dictionary, as shown in Table. 2.2.1.

For mechanical waves, the phrase "wave-function geometry" should not be interpreted as something intrinsically quantum. The eigenvector may describe unit-cell displacements, resonator amplitudes, wave polarizations, or rotor angles. The geometry comes from the fact that these internal patterns vary over the Brillouin zone. The Berry connection describes how to compare their phases. The quantum metric describes how quickly the internal pattern itself changes with momentum.

## 2.3. Wave topology: The Zak phase and the Chern number

### 2.3.1. The Zak phase as a holonomy

For a single isolated band, the Berry connection can be defined in analogy with the connection in differential geometry

$$A^{(n)}(k) = \mathrm{i}\,\langle u_n(k)|\partial_k u_n(k)\rangle\,. \tag{2.3.1}$$

I put the band index $n$ on the superscript to avoid confusion with the subindex from $k$. The Berry phase around the one-dimensional Brillouin zone is the Zak phase,

$$\gamma_n = \oint_{\mathrm{BZ}} A^{(n)}(k)\,\mathrm{d}k. \tag{2.3.2}$$

Under a gauge transformation

$$|u_n(k)\rangle \to e^{\mathrm{i}\chi(k)}\,|u_n(k)\rangle\,, \tag{2.3.3}$$

the Berry connection changes as

$$A_n(k) \to A_n(k) - \partial_k\chi(k), \tag{2.3.4}$$

so the Zak phase is defined modulo $2\pi$.

The important physical point is that this phase measures how the eigenvector twists as one moves around the entire Brillouin zone, a holonomy. In a mechanical or acoustic band, this means the relative amplitudes and phases of the degrees of freedom inside the unit cell may return to themselves only after acquiring a geometric phase.

In electronic systems, the Zak phase is related to the polarization and to the center of a Wannier orbital. In the wave problems discussed here, the analogous meaning is the center and phase winding of the band eigenmode within the unit cell. When inversion, chiral, or related symmetries are present, the Zak phase can be pinned to 0 or $\pi$ modulo $2\pi$. This quantized distinction is what makes the boundary physics robust: it cannot change continuously unless the bulk gap closes or the protecting symmetry is lost.

### 2.3.2. Extension to 2D: Berry curvature, Chern number, and gauge invariance

While the core focus of this lecture is on one-dimensional systems, the geometric framework of band bundles generalizes beautifully to higher dimensions, where it unlocks rich, intrinsically multi-dimensional topological phenomena. Consider a two-dimensional system where the crystal momentum becomes a vector $\mathbf{k} = (k_x, k_y)$, and the Brillouin zone BZ forms a two-dimensional torus $T^2$.

In this 2D setting, the Berry connection acts as a vector-like gauge potential with distinct components along each momentum axis:

$$A_{n,\mu}(\mathbf{k}) = \mathrm{i}\left\langle u_n(\mathbf{k})|\partial_{k_\mu} u_n(\mathbf{k})\right\rangle, \quad \mu \in \{x, y\}. \tag{2.3.5}$$

Under a smooth, local gauge transformation $|u_n(\mathbf{k})\rangle \to e^{\mathrm{i}\chi(\mathbf{k})}\,|u_n(\mathbf{k})\rangle$, each component transforms by picking up the gradient of the phase shift:

$$A_{n,\mu}(\mathbf{k}) \to A_{n,\mu}(\mathbf{k}) - \partial_{k_\mu}\chi(\mathbf{k}). \tag{2.3.6}$$

To construct a physical quantity free from this local gauge dependence, we compute the coordinate curl of this connection field. This defines the out-of-plane component of the *Berry curvature*:

$$\Omega_{n,xy}(\mathbf{k}) = \partial_{k_x} A_{n,y}(\mathbf{k}) - \partial_{k_y} A_{n,x}(\mathbf{k}). \tag{2.3.7}$$

If we evaluate how $\Omega_{n,xy}(\mathbf{k})$ transforms under a gauge rotation, the terms involving $\chi(\mathbf{k})$ cancel out identically because mixed partial derivatives of a smooth function commute ($\partial_{k_x}\partial_{k_y}\chi = \partial_{k_y}\partial_{k_x}\chi$). This leaves the Berry curvature *strictly gauge-invariant* at every single point in momentum space:

$$\Omega'_{n,xy}(\mathbf{k}) = \Omega_{n,xy}(\mathbf{k}). \tag{2.3.8}$$

Physically, $\Omega_{n,xy}(\mathbf{k})$ plays the role of an effective magnetic field threading the Brillouin zone, responsible for driving wave packets perpendicular to applied forces via an anomalous velocity.

Integrating this local gauge invariant over the entire closed 2D torus BZ yields the *first Chern number* $C_n$:

$$C_n = \frac{1}{2\pi}\int_{\mathrm{BZ}} \Omega_{n,xy}(\mathbf{k})\,\mathrm{d}k_x\mathrm{d}k_y. \tag{2.3.9}$$

Because the underlying integrand is perfectly gauge-invariant, the Chern number is an absolute global topological invariant ($\Delta C_n = 0$), contrasting with the 1D Zak phase which is only invariant modulo $2\pi$. By the Chern-Weil theorem, $C_n$ is strictly quantized to an integer ($C_n \in \mathbb{Z}$).

This contrast highlights a subtle nuance regarding Stokes' theorem. For a contractible loop $\mathcal{C}$ bounding a local disk-like region $S$ completely contained inside the BZ, Stokes' theorem applies cleanly:

$$\oint_{\mathcal{C}} \mathbf{A}_n \cdot \mathrm{d}\mathbf{k} = \int_S \Omega_{n,xy}\,\mathrm{d}k_x\mathrm{d}k_y. \tag{2.3.10}$$

Since the surface integral evaluates a strictly gauge-invariant field, the Berry phase around any such contractible loop is rigidly invariant.

However, for a non-contractible loop—like the line wrapping fully around a 1D Brillouin zone circle—the loop does not bound any surface *within* the BZ manifold. Without a valid bounding surface $S$ on the manifold, Stokes' theorem cannot be invoked. This topological freedom is precisely what allows a large gauge transformation to wind by a non-zero integer $m$ across the boundaries, shifting the Zak phase by $2\pi m$:

$$\chi(\pi/a) - \chi(-\pi/a) = 2\pi m, \quad m \in \mathbb{Z}. \tag{2.3.11}$$

When a 2D band bundle possesses a non-zero Chern number ($C_n \neq 0$), it implies that the eigenvectors are globally "twisted" over the torus. In this case, it is mathematically impossible to establish a single, smooth, continuous choice of gauge for $|u_n(\mathbf{k})\rangle$ across the entire BZ without encountering a phase singularity somewhere on the surface.

### 2.3.3. Quantum metric: distance between wave patterns

The Berry connection tells us about phase and parallel transport. The same family of eigenvectors also carries a metric. The metric answers a different question: how different are the internal wave patterns at two nearby momenta?

The gauge-invariant way to measure this distance is to remove the component of $\partial_k |u_n\rangle$ that only changes the phase of the eigenvector. Let

$$P_n(k) = |u_n(k)\rangle \langle u_n(k)| \tag{2.3.12}$$

be the projector onto the band. The one-dimensional quantum metric is

$$g_{kk}^{(n)} = \mathrm{Re}\,\langle \partial_k u_n| \left[1 - P_n(k)\right] |\partial_k u_n\rangle\,. \tag{2.3.13}$$

Equivalently, for two nearby normalized eigenmodes,

$$1 - |\langle u_n(k)|u_n(k+\mathrm{d}k)\rangle|^2 = g_{kk}^{(n)}\,\mathrm{d}k^2 + O(\mathrm{d}k^3). \tag{2.3.14}$$

Thus $g_{kk}\mathrm{d}k^2$ is the squared distance between two neighboring wave patterns, after ignoring the arbitrary gauge phase.

In higher dimensions, the same object is the quantum geometric tensor

$$T_{\mu\nu}^{(n)} = \left\langle \partial_{k_\mu} u_n \right| \left[1 - P_n(\boldsymbol{k})\right] \left|\partial_{k_\nu} u_n\right\rangle . \tag{2.3.15}$$

Its real part is the quantum metric,

$$g_{\mu\nu}^{(n)} = \mathrm{Re}\, T_{\mu\nu}^{(n)}, \tag{2.3.16}$$

and its imaginary part gives the Berry curvature,

$$F_{\mu\nu}^{(n)} = -2\,\mathrm{Im}\, T_{\mu\nu}^{(n)}. \tag{2.3.17}$$

So Berry curvature and quantum metric are not separate accidents. They are two parts of the same wave-function geometry.

### Take-home messages

1. **Band structure comes from reciprocal-space coupling.** In a periodic elastic medium, the material coefficients contain Fourier components at reciprocal-lattice vectors. These components couple plane waves whose wavevectors differ by reciprocal-lattice vectors:

   $$k \longleftrightarrow k - G. \tag{2.3.18}$$

   The central equation is the plane-wave representation of this coupling, and choosing one equivalence class $k = q + G$ gives the Bloch eigenvalue problem at fixed crystal momentum $q$.
2. **A Bragg gap is a two-wave avoided crossing.** Near a Bragg plane, two nearly degenerate waves are strongly coupled by the periodic modulation. Keeping only these two waves gives a $2 \times 2$ dynamical matrix. The gap is controlled by the Fourier component of the stiffness or density modulation that scatters one wave into the other.
3. **The same Bloch structure appears in many wave systems.** Elastic waves, acoustic waves, photonic crystals, electron bands, magnons, polaritons, plasmons, and mechanical metamaterials all lead to Bloch eigenvalue problems when the underlying coefficients are periodic. The microscopic fields differ, but the reciprocal-space bookkeeping is the same.
4. **Topology is carried by eigenvectors, not by eigenvalues.** The band dispersion $\omega_n(k)$ tells us the frequency of a wave, but the eigenvector $|u_n(k)\rangle$ tells us the wave pattern. As $k$ moves through the Brillouin zone, these eigenvectors form a band bundle. The phase freedom

   $$|u_n(k)\rangle \to e^{i\chi(k)}|u_n(k)\rangle \tag{2.3.19}$$

   is a gauge freedom, analogous to choosing a local frame in differential geometry.
5. **Berry connection, curvature, and metric are wave geometry.** The Berry connection describes how the phase of a Bloch eigenvector is compared between nearby momenta. In one dimension, its integral gives the Zak phase. In two dimensions, the Berry curvature and Chern number characterize the global twisting of the band bundle. The quantum metric measures something complementary: how rapidly the internal wave pattern itself changes with momentum, independent of arbitrary phase choice.

## Further reading


1. C. Kittel, *Introduction to Solid State Physics*, 8th ed., Wiley (2005). A standard reference for reciprocal lattices, Brillouin zones, band folding, and the central equation for waves in periodic media.
2. N. W. Ashcroft and N. D. Mermin, *Solid State Physics*, Holt, Rinehart and Winston (1976). A classic and detailed discussion of Bloch's theorem, reciprocal space, and band formation.
3. B. Simon, "Holonomy, the quantum adiabatic theorem, and Berry's phase," *Physical Review Letters* **51**, 2167–2170 (1983). A short and beautiful paper explaining Berry phase as holonomy in a fiber bundle.
4. T. Frankel, *The Geometry of Physics: An Introduction*, 3rd ed., Cambridge University Press (2012). A physics-oriented introduction to differential geometry, including vector bundles, connections, curvature, and gauge fields.
5. A. S. Sergeev, "Topological insulators and geometry of vector bundles," *SciPost Physics Lecture Notes* **67** (2023). A pedagogical lecture-note treatment of band eigenvectors as vector bundles, with emphasis on Berry geometry, holonomy, and the geometric origin of topological band phenomena.

## Homework 2: Band Structures and Wave Geometry

Lecture 2 introduced two complementary ideas. First, band structures arise because periodic media couple plane waves whose wavevectors differ by reciprocal-lattice vectors. Second, the Bloch eigenvectors themselves form a geometric object over the Brillouin zone, analogous to a vector bundle over a manifold.

### Problem 1: A discrete band structure with two sites per unit cell

Consider a one-dimensional mass-spring chain with two masses per unit cell. The displacement of the two masses in unit cell $n$ are $u_{A,n}$ and $u_{B,n}$. The masses are $m_A$ and $m_B$, and nearest neighbors are connected by identical springs of stiffness $K$. The equations of motion are

$$m_A \ddot{u}_{A,n} = -K(2u_{A,n} - u_{B,n} - u_{B,n-1}), \tag{2.3.20}$$

$$m_B \ddot{u}_{B,n} = -K(2u_{B,n} - u_{A,n} - u_{A,n+1}). \tag{2.3.21}$$

Use the Bloch form

$$u_{A,n}(t) = u_A(k)e^{i(kna-\omega t)}, \tag{2.3.22}$$

$$u_{B,n}(t) = u_B(k)e^{i(kna-\omega t)}, \tag{2.3.23}$$

where $a$ is the unit-cell length.

1. Show that the equations of motion become the generalized Bloch eigenvalue problem

$$K \begin{pmatrix} 2 & -(1+e^{-ika}) \\ -(1+e^{ika}) & 2 \end{pmatrix} \begin{pmatrix} u_A \\ u_B \end{pmatrix} = \omega^2 \begin{pmatrix} m_A & 0 \\ 0 & m_B \end{pmatrix} \begin{pmatrix} u_A \\ u_B \end{pmatrix}. \tag{2.3.24}$$

2. Derive the two bands

$$\omega_{\pm}^2(k) = \frac{K(m_A+m_B)}{m_A m_B} \pm \frac{K}{m_A m_B}\sqrt{(m_A+m_B)^2 - 4m_A m_B \sin^2\frac{ka}{2}}. \tag{2.3.25}$$

3. Show that the lower branch is acoustic at small $k$:

$$\omega_-^2(k) \simeq \frac{Ka^2}{2(m_A+m_B)}k^2. \tag{2.3.26}$$

   Explain physically why this mode corresponds to the two masses moving nearly in phase.

4. At $k = 0$, identify the qualitative motion of the upper branch. Show that it is an optical-like mode in which the two masses move oppositely, with approximately no center-of-mass motion:

$$m_A u_A + m_B u_B = 0. \tag{2.3.27}$$

5. Evaluate the two values of $\omega^2$ at the Brillouin-zone edge $k = \pi/a$. Show that the gap in $\omega^2$ is

$$\Delta(\omega^2) = \frac{2K|m_A - m_B|}{m_A m_B}. \tag{2.3.28}$$

6. Discuss the special case $m_A = m_B$. Why does the zone-edge gap close? Explain why, in this case, the two-band description is partly a consequence of choosing a larger unit cell: the original monatomic chain dispersion has been folded into a smaller Brillouin zone.
7. Compare this problem with the Bragg-gap discussion in Lecture 2. What is the shared Bloch-matrix structure? What is physically different about the origin of the two branches and the gap?

**Problem 2: Differential geometry and wave geometry**

In Lecture 2, a single isolated Bloch band was described as a vector bundle over the Brillouin zone. In one dimension, the base space is the circle

$$k \in \mathrm{BZ} \simeq S^1. \tag{2.3.29}$$

At each $k$, the fiber is the one-dimensional space spanned by the normalized Bloch eigenvector $|u(k)\rangle$.

Consider the following family of normalized two-component wave patterns:

$$|u(k)\rangle = \frac{1}{\sqrt{2}} \begin{pmatrix} 1 \\ e^{i\phi(k)} \end{pmatrix}, \qquad \phi(k + 2\pi/a) = \phi(k) + 2\pi N, \tag{2.3.30}$$

where $N$ is an integer.

1. In the language of differential geometry, identify the analogs of the following objects:

   base space, fiber, local section, gauge transformation, connection. (2.3.31)

2. Compute the Berry connection

   $$A(k) = i\langle u(k)|\partial_k u(k)\rangle. \tag{2.3.32}$$

3. Compute the Zak phase

   $$\gamma_{\mathrm{Zak}} = \oint_{\mathrm{BZ}} A(k)\, dk. \tag{2.3.33}$$

   Express your answer in terms of the winding number $N$.

4. Now perform a gauge transformation

   $$|u(k)\rangle \to e^{i\chi(k)}|u(k)\rangle. \tag{2.3.34}$$

   Show how $A(k)$ changes. Explain why $\gamma_{\mathrm{Zak}}$ is only defined modulo $2\pi$.

# Lecture 3: Wave Topology and Topological Mechanics

**Overview.** Lecture 2 introduced Bloch waves as momentum-space eigenvalue problems and emphasized that the eigenvectors themselves carry geometry through the Berry connection, Zak phase, Berry curvature, and quantum metric. This lecture turns that geometric language into topology and boundary physics. We begin with the elastic SSH chain, a clean full-Brillouin-zone model in which the off-diagonal Bloch function traces a closed loop in the complex plane. This loop gives a winding number, and the corresponding Zak phase predicts an interface mode when two dimerization patterns meet. We then reinterpret the continuum Bragg theory from Lecture 2 as the local Dirac expansion near the SSH gap closing: it is not by itself a full-BZ topological invariant, but it is the natural envelope theory for a mass domain wall and its localized mode. The second half of the lecture shifts from ordinary band topology to Maxwell topology. In Maxwell lattices the central object is not the finite-frequency phonon eigenvector, but the compatibility matrix $C$, which maps displacements to bond extensions. Its winding, or equivalently the topology of the chiral square-root Hamiltonian built from $C$, controls zero modes and states of self-stress. The rotor chain provides the minimal example, showing explicitly how geometry determines the constraint map, how its winding predicts an edge zero mode, and how zero modes and states of self-stress are dual. The main message is that ordinary band topology classifies wave eigenvectors, while Maxwell topology classifies mechanical constraints.

## 3.1. Elastic SSH chain: the clean full-BZ winding model

The continuum Bragg problem from Lecture 2 is very useful for deriving a local gap-opening Hamiltonian near a Bragg plane. However, it is a local theory near one point in the Brillouin zone. To demonstrate the physics of the Zak phase, we want a model whose Bloch eigenvectors are analytically defined around the entire Brillouin zone. The cleanest mechanical example is the Su–Schrieffer–Heeger (SSH) chain made from alternating springs. It is a discrete "tight-binding" version of the more general continuum problem, and we discuss more abotu their relations in Sec. 3.2.1.

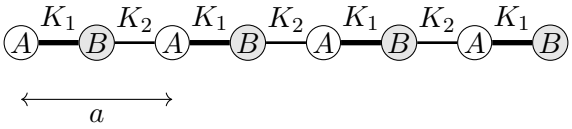


Figure 6: SSH chain: two sites (A, B) per unit cell and alternating spring constants $(K_1, K_2)$.

Consider a one-dimensional chain with two identical masses per unit cell 6. Let their displacements be $u_{A,n}$ and $u_{B,n}$, where $n$ labels the unit cell. The spring $K_1$ connects $A_n$ to $B_n$, while the spring $K_2$ connects $B_n$ to $A_{n+1}$. The equations of motion are

$$m\ddot{u}_{A,n} = -K_1(u_{A,n} - u_{B,n}) - K_2(u_{A,n} - u_{B,n-1}), \tag{3.1.1}$$

$$m\ddot{u}_{B,n} = -K_1(u_{B,n} - u_{A,n}) - K_2(u_{B,n} - u_{A,n+1}). \tag{3.1.2}$$

Using the Bloch form

$$\begin{pmatrix} u_{A,n} \\ u_{B,n} \end{pmatrix} = \begin{pmatrix} u_A(k) \\ u_B(k) \end{pmatrix} e^{\mathrm{i}kna} e^{-\mathrm{i}\omega t}, \tag{3.1.3}$$

we obtain

$$D(k) \begin{pmatrix} u_A(k) \\ u_B(k) \end{pmatrix} = \omega^2 \begin{pmatrix} u_A(k) \\ u_B(k) \end{pmatrix}, \tag{3.1.4}$$

with

$$D(k) = \frac{1}{m} \begin{pmatrix} K_1 + K_2 & -K_1 - K_2 e^{-\mathrm{i}ka} \\ -K_1 - K_2 e^{\mathrm{i}ka} & K_1 + K_2 \end{pmatrix}. \tag{3.1.5}$$

The diagonal term $(K_1 + K_2)/m$ only shifts the value of $\omega^2$. The topology is controlled by the off-diagonal part. After subtracting this common shift and ignoring an overall sign, define the chiral two-band hamiltonian

$$h_{\mathrm{SSH}}(k) = \begin{pmatrix} 0 & K_1 + K_2 e^{-\mathrm{i}ka} \\ K_1 + K_2 e^{\mathrm{i}ka} & 0 \end{pmatrix}. \tag{3.1.6}$$

Here SSH refers to Su–Schrieffer–Heeger, whose seminal paper on electronic structures of polyacetylene first revealed this type of topology. This has the standard form

$$h_{\mathrm{SSH}}(k) = d_x(k)\sigma_x + d_y(k)\sigma_y, \qquad \{\sigma_z, h_{\mathrm{SSH}}(k)\} = 0, \tag{3.1.7}$$

where

$$d_x(k) = K_1 + K_2 \cos ka, \tag{3.1.8}$$

$$d_y(k) = K_2 \sin ka. \tag{3.1.9}$$

Equivalently,

$$d_x(k) + \mathrm{i}d_y(k) = K_1 + K_2 e^{\mathrm{i}ka}. \tag{3.1.10}$$

This is the key simplification. As $k$ winds once around the Brillouin zone, the complex number $K_1 + K_2 e^{\mathrm{i}ka}$ traces a circle centered at $(K_1, 0)$ with radius $K_2$. Thus the topological question becomes a simple geometric question: does this circle enclose the origin?

To solve for the eigenvectors and analyze the geometry and topology, we write

$$d_x(k) + \mathrm{i}d_y(k) = |d(k)| e^{\mathrm{i}\phi(k)}. \tag{3.1.11}$$

The eigenvectors are

$$|u_\pm(k)\rangle = \frac{1}{\sqrt{2}} \begin{pmatrix} 1 \\ \pm e^{\mathrm{i}\phi(k)} \end{pmatrix}. \tag{3.1.12}$$

with corresponding eigenvalues

$$\lambda_\pm(k) = \pm|d(k)| = \pm|K_1 + K_2 e^{\mathrm{i}ka}|, \tag{3.1.13}$$

so the actual spring-chain frequencies are

$$\omega_\pm^2(k) = \frac{K_1 + K_2}{m} \mp \frac{|K_1 + K_2 e^{\mathrm{i}ka}|}{m}, \tag{3.1.14}$$

where the sign convention reflects the overall minus sign relating the physical dynamical matrix to $h_{\mathrm{SSH}}$. The band gap closes only when

$$K_1 = K_2, \qquad k = \frac{\pi}{a}. \tag{3.1.15}$$

Therefore $K_1 = K_2$ is the topological transition point. The two gapped phases are distinguished by whether the strong spring lies inside the unit cell or between neighboring unit cells.

### 3.2. Zak phase, winding, and the SSH interface mode

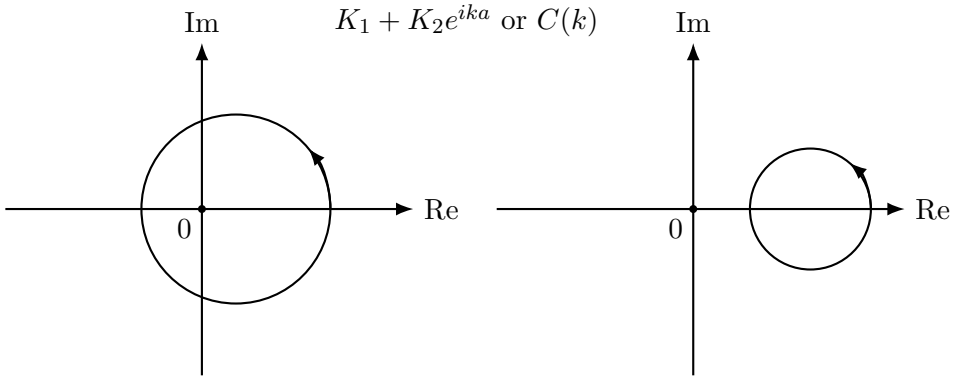


Figure 7: The winding of $|d(k)|e^{i\phi(k)} = K_1 + K_2 e^{ika}$ (or $C(k)$ for Maxwell lattices discussed in later sections) over the first Brillouin zone. $N_w = 1$ ($K_2 > K_1$) on the left and $N_w = 0$ ($K_2 < K_1$) on the right. For the case of Maxwell lattices, this correspond to $|c_2| > |c_1|$ and $|c_2| < |c_1|$.

We can then compute the Berry connection we introduced in the last class. If we pick the lower band, it is

$$A(k) = \mathrm{i}\,\langle u_-(k)|\partial_k u_-(k)\rangle \tag{3.2.1}$$

$$= -\frac{1}{2}\partial_k \phi(k). \tag{3.2.2}$$

Note the factor of $1/2$ comes from the fact that the SSH eigenstate is a two-component wave function with equal weight on the two sublattices (A and B). This is very important. As we see below, when $\phi(k)$ winds by $2\pi$, the eigenvector winds by $\pi$: it only picks up half of that winding in its Berry phase. The deeper way to say it is that $u_\pm(k)$ is a spinor field of a spin$-1/2$ particle.

Hence the Zak phase is

$$\gamma_{\mathrm{Zak}} = \oint_{\mathrm{BZ}} A(k)\,\mathrm{d}k \tag{3.2.3}$$

$$= -\frac{1}{2}\oint_{\mathrm{BZ}} \partial_k \phi(k)\,\mathrm{d}k \tag{3.2.4}$$

$$= -\pi N_w \qquad \mod 2\pi, \tag{3.2.5}$$

where

$$N_w = \frac{1}{2\pi}\oint_{\mathrm{BZ}} \partial_k \phi(k)\,\mathrm{d}k. \tag{3.2.6}$$

For the SSH spring chain,

$$e^{\mathrm{i}\phi(k)} = \frac{K_1 + K_2 e^{\mathrm{i}ka}}{|K_1 + K_2 e^{\mathrm{i}ka}|}. \tag{3.2.7}$$

Therefore

$$K_2 > K_1 \quad \Rightarrow \quad N_w = 1, \qquad \gamma_{\mathrm{Zak}} = \pi \mod 2\pi, \tag{3.2.8}$$

$$K_2 < K_1 \quad \Rightarrow \quad N_w = 0, \qquad \gamma_{\mathrm{Zak}} = 0 \mod 2\pi. \tag{3.2.9}$$

The first case is topological for the unit-cell convention used in Fig. 6: the stronger spring connects neighboring unit cells. The second case is trivial: the stronger spring forms isolated dimers inside the unit cell.

Crucially, this distinction predicts a boundary or interface mode, a relation called "bulk-boundary correspondence." To see this in a simple way, consider an open chain in the topological limit $K_2 > K_1$. At the middle of the shifted gap, the chiral equation reduces to

$$h_{\mathrm{SSH}}\boldsymbol{u} = 0. \tag{3.2.10}$$

Note we are considering the real space version of this equation, which means translating $h_{\mathrm{SSH}}$ back to real space (dropping diagonal terms) and consider the middle of the shifted gap.

A left-localized mode can be chosen to live only on one sublattice, say $u_{B,n} = 0$. The remaining equation gives the recurrence relation

$$K_1 u_{A,n} + K_2 u_{A,n+1} = 0, \tag{3.2.11}$$

so

$$u_{A,n+1} = -\frac{K_1}{K_2} u_{A,n}. \tag{3.2.12}$$

This mode is normalizable precisely when

$$\left|\frac{K_1}{K_2}\right| < 1, \tag{3.2.13}$$

which is the same condition as the nonzero winding. In the physical spring chain this mode appears near the midgap frequency

$$\omega^2 = \frac{K_1 + K_2}{m}, \tag{3.2.14}$$

because zero energy in the shifted chiral matrix corresponds to the middle of the spring-chain band gap.

An interface between two dimerizations works the same way. If the left side has $K_2 > K_1$ and the right side has $K_2 < K_1$ in a common unit-cell convention, the winding number changes by one across the interface. The interface must bind a localized mode in the gap. This is the one-dimensional bulk–edge correspondence in its simplest mechanical form. A numerical example is shown in Fig. 8.

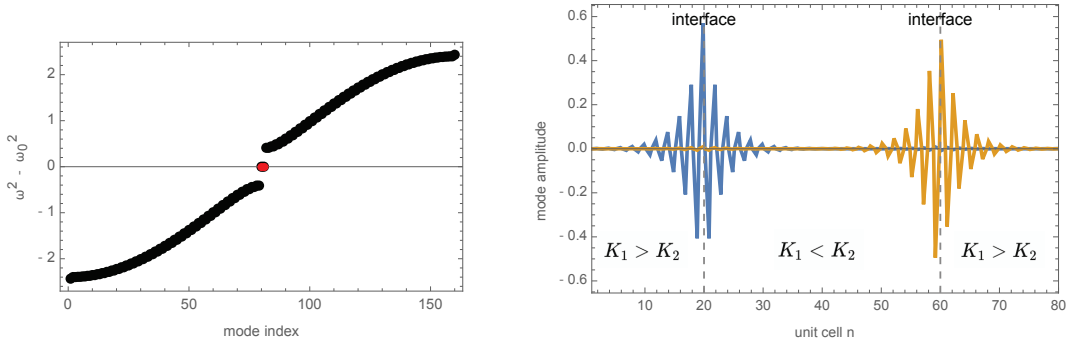


Figure 8: Spectrum (left) and interface modes (right) of the SSH chain defined in Fig. 6. We simulated a chain of 80 sites, with interfaces at 20 and 60. The red dots in the spectrum plot are the interface modes.

### 3.2.1. Continuum Bragg theory as the local Dirac limit

In this subsection, we connect the SSH chain we just talked about with the continuum waves we discussed in Lecture 2. We show that they share the same structure near the Bragg plane ($k = G/2 = \pi/a$), and thus are governed by the same wave topology, although the continuum wave problem can't be analytically solved in the entire Brillouin zone to show the Zak phase in a clean way.

Expand the SSH loop near the transition point

$$K_1 \approx K_2, \qquad k = \frac{\pi}{a} + q, \qquad |qa| \ll 1. \tag{3.2.15}$$

Then

$$K_1 + K_2 e^{\mathrm{i}ka} = K_1 - K_2 e^{\mathrm{i}qa} \tag{3.2.16}$$

$$\approx (K_1 - K_2) - \mathrm{i}K_2 aq. \tag{3.2.17}$$

Thus the SSH Hamiltonian reduces locally to

$$h(q) \approx (K_1 - K_2)\sigma_x - K_2 aq\, \sigma_y. \tag{3.2.18}$$

This is a one-dimensional Dirac Hamiltonian. The mass term is

$$m_{\mathrm{SSH}} = K_1 - K_2, \tag{3.2.19}$$

so the topological transition occurs when the mass changes sign.

Now compare this with the continuum Bragg problem from Lecture 2. Consider the scalar elastic wave equation

$$-\frac{\mathrm{d}}{\mathrm{d}x}\left[E(x)\frac{\mathrm{d}u}{\mathrm{d}x}\right] = \rho_0\omega^2 u, \tag{3.2.20}$$

with

$$E(x) = E_0 + U_G e^{\mathrm{i}Gx} + U_G^* e^{-\mathrm{i}Gx}, \qquad U_G = E_c - \mathrm{i}E_s. \tag{3.2.21}$$

Near the first Bragg plane, the two nearly degenerate traveling waves are

$$k_+ = \frac{G}{2} + q, \qquad k_- = -\frac{G}{2} + q. \tag{3.2.22}$$

Projecting the elastic operator into this two-wave subspace gives, to leading order in $q$ and in the weak modulation,

$$\mathcal{D}_{\mathrm{tr}}(q) = \omega_B^2 \mathbb{I} + \begin{pmatrix} 2\omega_B v_0 q & \Delta \\ \Delta^* & -2\omega_B v_0 q \end{pmatrix}, \tag{3.2.23}$$

where

$$v_0 = \sqrt{E_0/\rho_0}, \qquad \omega_B = \frac{v_0 G}{2}, \tag{3.2.24}$$

while the Bragg coupling is linear in the Fourier component of the modulus,

$$\Delta = -\frac{G^2}{4\rho_0} U_G = -\frac{G^2}{4\rho_0}(E_c - \mathrm{i}E_s). \tag{3.2.25}$$

Therefore, if

$$\Delta = \Delta_x - \mathrm{i}\Delta_y, \tag{3.2.26}$$

then

$$\Delta_x = -\frac{G^2}{4\rho_0} E_c, \tag{3.2.27}$$

$$\Delta_y = -\frac{G^2}{4\rho_0} E_s. \tag{3.2.28}$$

After subtracting the common Bragg frequency, the local two-wave matrix is

$$h_{\mathrm{tr}}(q) = \Delta_x \sigma_x + \Delta_y \sigma_y + 2\omega_B v_0 q\, \sigma_z. \tag{3.2.29}$$

For a fixed modulation phase, we may choose the origin of the unit cell so that $\Delta$ is real. Then

$$h_{\mathrm{tr}}(q) = \Delta \sigma_x + 2\omega_B v_0 q\, \sigma_z. \tag{3.2.30}$$

A fixed basis rotation,

$$R = e^{\mathrm{i}\pi\sigma_x/4}, \tag{3.2.31}$$

maps $\sigma_z$ to $\sigma_y$ while leaving $\sigma_x$ unchanged. Thus

$$h(q) = R h_{\mathrm{tr}}(q) R^\dagger = \Delta \sigma_x + 2\omega_B v_0 q\, \sigma_y. \tag{3.2.32}$$

This has exactly the same form as the SSH Dirac expansion in Eq. (3.2.18). The continuum Bragg mass $\Delta$ plays the same role as $K_1 - K_2$.

The important distinction is global versus local. The continuum Bragg Hamiltonian

$$h(q) = \Delta \sigma_x + 2\omega_B v_0 q\, \sigma_y \tag{3.2.33}$$

only gives a line in the $(d_x, d_y)$ plane as $q$ varies. By itself, this line is not a closed loop around the Brillouin zone. Therefore it is not the most natural object for defining the Zak phase. Instead, it tells us what happens near the gap closing point of a full periodic model, such as the SSH chain.

It is nevertheless the right language for the interface mode. Let the mass vary slowly in space,

$$\Delta \to \Delta(x), \qquad q \to -\mathrm{i}\partial_x. \tag{3.2.34}$$

At the middle of the Bragg gap, $\omega^2 = \omega_B^2$, the envelope equation is

$$[\Delta(x)\sigma_x - \mathrm{i}2\omega_B v_0 \sigma_y \partial_x]\, \boldsymbol{\psi}(x) = 0. \tag{3.2.35}$$

Writing $\boldsymbol{\psi} = (\psi_1, \psi_2)^T$, this gives

$$[\Delta(x) - 2\omega_B v_0 \partial_x]\, \psi_2(x) = 0, \tag{3.2.36}$$

$$[\Delta(x) + 2\omega_B v_0 \partial_x]\, \psi_1(x) = 0. \tag{3.2.37}$$

If

$$\Delta(x) < 0 \quad (x < 0), \qquad \Delta(x) > 0 \quad (x > 0), \tag{3.2.38}$$

one normalizable solution has $\psi_2 = 0$ and

$$\psi_1(x) = \psi_1(0) \exp\left[ -\int_0^x \frac{\Delta(x')}{2\omega_B v_0}\, \mathrm{d}x' \right]. \tag{3.2.39}$$

If the sign change is reversed, the localized solution lives in the other chiral component. Thus the continuum Bragg model is the local domain-wall theory of the SSH transition.

## 3.3. Maxwell lattices: topology of constraints

Now we shift our gears to a different type of topological waves in mechanical systems: Maxwell lattice topological mechanics. Here, the topological modes are zero modes, characterizing soft motion and self stress, making these lattices particularly interesting for the control of static and low frequency mechanical properties.

A mechanical network with small displacements $u$ and bond extensions $e$ is described by a compatibility matrix

$$e = Cu. \tag{3.3.1}$$

The dimension of the $C$ matrix is $N_b \times N_s d$ where $N_b$ is the number of the bonds, $N_s$ is the number of the sites, and $d$ is the spatial dimension. The dual object is the equilibrium matrix $Q$, which maps bond tensions $t$ to forces $f$ on sites,

$$f = Qt. \tag{3.3.2}$$

For ordinary central-force systems,

$$Q = C^\dagger, \tag{3.3.3}$$

up to conventions and possible metric factors.

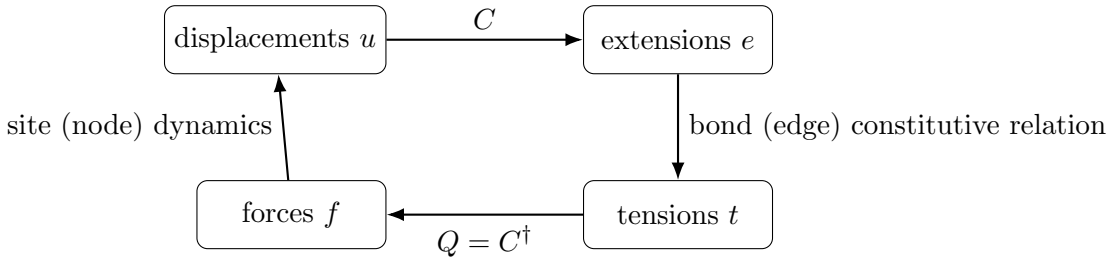


Figure 9: Compatibility and equilibrium maps between site space (left) bond space (right).

The zero modes (ZMs) are displacement patterns that stretch no bonds:

$$Cu = 0. \tag{3.3.4}$$

The states of self-stress (SSSs) are tension patterns that produce no net forces:

$$Qt = 0. \tag{3.3.5}$$

These are different null spaces:

$$\text{zero modes}: \quad \ker C, \qquad \text{states of self-stress}: \quad \ker Q. \tag{3.3.6}$$

We use $N_0, N_{SSS}$ to denote the dimensions of these null spaces.

### 3.3.1. Maxwell–Calladine relation

Applying rank-nullity theorem to the $Q, C$ matrices, we get the Maxwell–Calladine relation, which states that

$$N_0 - N_{\text{SSS}} = N_{\text{dof}} - N_b, \tag{3.3.7}$$

where $N_0$ is the number of zero modes, $N_{\mathrm{SSS}}$ is the number of states of self-stress, $N_{\mathrm{dof}}$ is the number of mechanical degrees of freedom ($N_{\mathrm{dof}} = N_s d$ in the simple spring-mass problems we discuss here but can be more general), and $N_b$ is the number of constraints or bonds.

Maxwell lattices are defined as lattices where in the bulk,

$$N_{\mathrm{dof}} = N_b. \tag{3.3.8}$$

Then the index vanishes in the periodic bulk:

$$N_0 = N_{\mathrm{SSS}}. \tag{3.3.9}$$

However, this equality does not say where zero modes and states of self-stress are located. Topology determines their spatial distribution. Maxwell counting tells us the difference between zero modes and states of self-stress. Maxwell topology tells us how they are polarized toward boundaries and defects.

## 3.4. Topological invariant of a Maxwell lattice

For a periodic Maxwell lattice, Fourier transform the compatibility matrix,

$$C \to C(k). \tag{3.4.1}$$

For an isostatic lattice, $C(k)$ is square in the bulk. If

$$\det C(k) \neq 0 \tag{3.4.2}$$

throughout the Brillouin zone, the bulk has no nontrivial zero modes at finite $k$, and one can define a winding number. This is the direct Maxwell-lattice analog of the SSH winding, but it is a winding of the constraint map rather than a winding of the ordinary phonon eigenvectors.

A useful way to connect this statement to the Berry connection and Zak phase is to form the chiral Hamiltonian

$$H_M(k) = \begin{pmatrix} 0 & C^\dagger(k) \\ C(k) & 0 \end{pmatrix}. \tag{3.4.3}$$

This Hamiltonian acts on the enlarged space of displacement-like variables and bond-tension-like variables. Its square is block diagonal,

$$H_M^2(k) = \begin{pmatrix} C^\dagger(k)C(k) & 0 \\ 0 & C(k)C^\dagger(k) \end{pmatrix}, \tag{3.4.4}$$

contains the ordinary dynamical matrix $D(k) = C^\dagger(k)C(k)$. Thus the nonzero spectrum of $H_M$ is the square root of the usual mechanical spectrum, while its zero modes include both displacement zero modes and states of self-stress. This is the "square-root" construction used by Kane and Lubensky to relate isostatic mechanics to topological band theory.

The topological invariant can now be written in a form that looks very close to the SSH/Zak-phase discussion. In one dimension,

$$\nu_M = \frac{1}{2\pi \mathrm{i}} \oint_{\mathrm{BZ}} \mathrm{d}k \, \partial_k \log \det C(k). \tag{3.4.5}$$

Equivalently, writing

$$\det C(k) = |\det C(k)| e^{\mathrm{i}\Phi(k)}, \tag{3.4.6}$$

one has

$$\nu_M = \frac{1}{2\pi} \oint_{\mathrm{BZ}} \partial_k \Phi(k) \, \mathrm{d}k. \tag{3.4.7}$$

The phase $\Phi(k)$ is therefore the Maxwell counterpart of the SSH phase $\phi(k) = \arg[d_x(k) + \mathrm{i}d_y(k)]$.

### 3.5. Rotor chain as the minimal Maxwell example

Next we discuss the rotor chain as a simple one-dimensional Maxwell model. Each unit cell contains one rigid rotor with small angular displacement $\theta_j$. Neighboring rotors are connected by a spring or linkage. The important point for the lecture is that the linear coefficients come from geometry.

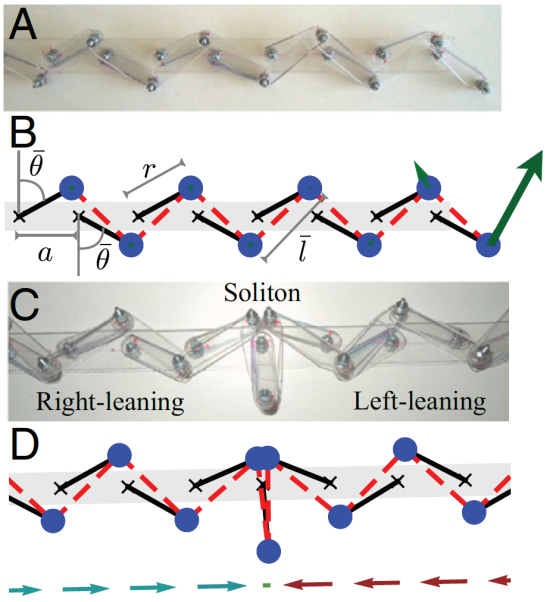


Figure 10: Topological Maxwell rotor chain.

A convenient geometric description is the following. The bond $j$ connects an attachment point on rotor $j$ to an attachment point on rotor $j+1$. Let $\hat{\ell}$ be the equilibrium unit vector along the linkage, and let $\boldsymbol{a}$ and $\boldsymbol{b}$ be the two equilibrium lever-arm vectors from the neighboring pivots to the attachment points. A small rotation gives attachment-point displacements

$$\delta \boldsymbol{r}_A = \theta_j \, \hat{\boldsymbol{z}} \times \boldsymbol{a}, \qquad \delta \boldsymbol{r}_B = \theta_{j+1} \, \hat{\boldsymbol{z}} \times \boldsymbol{b}. \tag{3.5.1}$$

Projecting the relative displacement onto the linkage direction gives

$$e_j = \hat{\ell} \cdot (\delta \boldsymbol{r}_B - \delta \boldsymbol{r}_A) = c_1 \theta_j + c_2 \theta_{j+1}, \tag{3.5.2}$$

with

$$c_1 = -\hat{\ell} \cdot (\hat{\boldsymbol{z}} \times \boldsymbol{a}), \qquad c_2 = \hat{\ell} \cdot (\hat{\boldsymbol{z}} \times \boldsymbol{b}). \tag{3.5.3}$$

Thus $c_1$ and $c_2$ are geometric lever arms determined by the equilibrium rotor angle, attachment geometry, and unit-cell choice.

This is a Maxwell chain: there is one degree of freedom and one constraint per unit cell in the periodic bulk.

Fourier transforming with

$$\theta_j = \theta(k) e^{\mathrm{i}kja}, \tag{3.5.4}$$

one obtains

$$e(k) = C(k)\theta(k), \tag{3.5.5}$$

with

$$C(k) = c_1 + c_2 e^{\mathrm{i}ka}. \tag{3.5.6}$$

The Maxwell winding is

$$\nu_M = \frac{1}{2\pi \mathrm{i}} \oint_{\mathrm{BZ}} \mathrm{d}k \, \partial_k \log\left(c_1 + c_2 e^{\mathrm{i}ka}\right). \tag{3.5.7}$$

As $k$ winds around the Brillouin zone, $C(k)$ traces a circle in the complex plane centered at $c_1$ with radius $|c_2|$. Therefore,

$$\nu_M = 0, \qquad |c_1| > |c_2|, \tag{3.5.8}$$

and

$$\nu_M = 1, \qquad |c_2| > |c_1|, \tag{3.5.9}$$

again up to orientation and unit-cell conventions. The topological transition occurs when

$$|c_1| = |c_2|, \tag{3.5.10}$$

where $C(k)$ vanishes at some momentum and the bulk develops a zero mode.

### 3.5.1. Edge zero mode

For an open chain, a zero mode satisfies

$$e_j = 0 \tag{3.5.11}$$

for every bond. Using Eq. (3.5.2), this gives

$$c_1\theta_j + c_2\theta_{j+1} = 0, \tag{3.5.12}$$

or

$$\theta_{j+1} = -\frac{c_1}{c_2}\theta_j. \tag{3.5.13}$$

Thus

$$\theta_j = \left(-\frac{c_1}{c_2}\right)^{j-1} \theta_1. \tag{3.5.14}$$

This mode is localized near the left edge when

$$\left|\frac{c_1}{c_2}\right| < 1. \tag{3.5.15}$$

For the opposite parameter regime, the corresponding zero mode is localized near the other edge, after choosing the appropriate termination.

### 3.5.2. States of self-stress

The equilibrium equation is the dual problem. Bond tensions $t_j$ generate torques on rotor $j$ of the form

$$\tau_j = c_1 t_j + c_2 t_{j-1}, \tag{3.5.16}$$

with boundary conventions depending on the termination. A state of self-stress satisfies

$$Qt = 0, \tag{3.5.17}$$

so in the bulk

$$c_1 t_j + c_2 t_{j-1} = 0, \tag{3.5.18}$$

or

$$t_j = -\frac{c_2}{c_1} t_{j-1}. \tag{3.5.19}$$

This recurrence is dual to the zero-mode recurrence. Thus zero modes and states of self-stress are naturally polarized in opposite ways.

### 3.6. Maxwell topological modes in higher dimensions and beyond

The physics we discussed above is not limited to 1D chains. We can extend the winding number to 2D and 3D lattices. For example, for a 2D lattice defined on a Bravais lattice

$$\vec{R} = n_1\vec{a}_1 + n_2\vec{a}_2 \tag{3.6.1}$$

we have $k$ space spanned by the two reciprocal lattice vectors

$$\vec{k} = k_1\vec{b}_1 + k_2\vec{b}_2, \tag{3.6.2}$$

with the first Brillouin zone defined in the usual way.

We have separate winding numbers

$$\begin{aligned}\nu_{M,1}(k_2) &= \frac{1}{2\pi\mathrm{i}}\oint_{\mathrm{BZ}} \mathrm{d}k_1\, \partial_{k_1} \log\det C(k_1,k_2),\\ \nu_{M,2}(k_1) &= \frac{1}{2\pi\mathrm{i}}\oint_{\mathrm{BZ}} \mathrm{d}k_2\, \partial_{k_2} \log\det C(k_1,k_2).\end{aligned} \tag{3.6.3}$$

It is worth noting that the winding number for direction $\vec{a}_1$ is a function of $k_2$ and vice versa. Importantly, these indices are not defined for $\nu_{M,1}(k_2 = 0)$ or $\nu_{M,2}(k_1 = 0)$ because $\vec{k} = 0$ is a gap-closing point due to the Nambu-Goldstone theorem.

For simple lattices such as the topological kagome lattice, $\nu_{M,1}(k_2)$ is a constant for all $k_2 \neq 0$, $\nu_{M,2}(k_1)$ is a constant for all $k_1 \neq 0$, and we can simply call them $\nu_{M,1}$ and $\nu_{M,2}$. In this case, a global topological polarization vector can be defined

$$\vec{R} = \nu_{M,1}\vec{a}_1 + \nu_{M,2}\vec{a}_2, \tag{3.6.4}$$

controlling ZM and SSS localization at boundaries and interfaces. There are also lattices when these are not constants, giving rise to Weyl points, and opposite polarization for waves with long and short wavelength along the boundary.

Furthermore, the topological mechanical phenomena in Maxwell lattices can also be extended to continuum elasticity with a modified winding number, disordered networks, quasi-periodic lattices, out-of-plane modes of thin-sheet metamaterials, etc. These are beyond the scope of this lecture. I show some examples of these systems in Fig. 11. These effects are useful in many technologies, offering polarized elasticity, wave guiding and stress-focusing.

### Take-home messages

1. **Topology is global wave geometry.** Lecture 2 introduced the Berry connection, Zak phase, and band bundle. Lecture 3 shows how these geometric quantities become topological when they are quantized by symmetry. A topological invariant cannot change under a smooth deformation unless the bulk gap closes or the protecting symmetry is broken.
2. **The SSH chain as the cleanest one-dimensional winding model.** For the elastic SSH chain, after subtracting the common diagonal shift, the topology is controlled by the off-diagonal Bloch function $K_1 + K_2e^{ika}$. As $k$ winds around the Brillouin zone, it traces a closed loop in the complex plane. Whether this loop encloses the origin distinguishes the two dimerized phases. The Zak phase measures (1/2 times) this winding using the wave geometry language on the eigenvectors. Connecting two domains of different Zak phase causes a topological interface mode, controlled by the bulk-boundary correspondence.

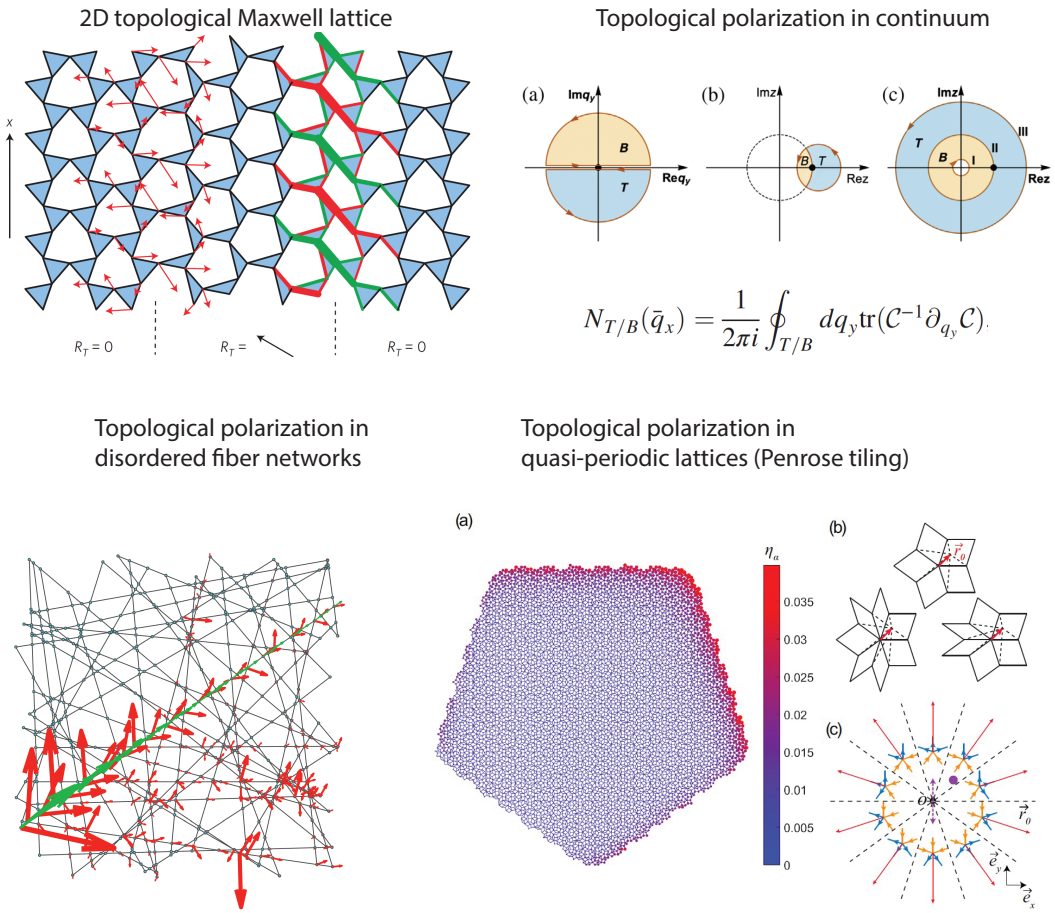


Figure 11: More Maxwell lattice topological mechanics examples.

3. **The continuum Bragg theory is the local Dirac limit.** The two-wave Bragg model near a zone-edge gap has the same local structure as the SSH chain near its transition:

$$h(q) = m\sigma_x + vq\,\sigma_y. \tag{3.6.5}$$

A sign change of the mass $m$ gives a Jackiw–Rebbi-type domain-wall mode. However, this continuum Dirac theory is local in momentum space. By itself, it does not define a full Brillouin-zone winding; it should be understood as the long-wavelength theory near a topological transition.

4. **Maxwell topology is topology of constraints, not ordinary bands.** In Maxwell lattices, the central object is the compatibility matrix

$$e = Cu, \tag{3.6.6}$$

which maps displacements to bond extensions. For an isostatic lattice, $C(k)$ is square in the bulk, and its winding defines a topological invariant:

$$\nu_M = \frac{1}{2\pi i}\oint_{\mathrm{BZ}} dk\,\partial_k \log\det C(k). \tag{3.6.7}$$

This invariant classifies zero modes and states of self-stress, rather than finite-frequency phonon eigenvectors.

5. **Zero modes and states of self-stress are dual.** The compatibility matrix $C$ and equilibrium matrix $Q = C^\dagger$ define two dual null spaces:

$$\text{zero modes} : \ker C, \qquad \text{states of self-stress} : \ker Q. \tag{3.6.8}$$

Maxwell–Calladine counting fixes the difference between their numbers, while topology controls where they are localized.

## Further reading


1. W. P. Su, J. R. Schrieffer, and A. J. Heeger, "Solitons in polyacetylene," *Physical Review Letters* **42**, 1698–1701 (1979). The original SSH paper. This is the historical source of the alternating-bond chain, the two dimerized phases, and the soliton/domain-wall bound state.
2. J. K. Asbóth, L. Oroszlány, and A. Pályi, *A Short Course on Topological Insulators*, Lecture Notes in Physics **919**, Springer (2016). A very pedagogical introduction to the SSH chain, winding number, Zak phase, and bulk-boundary correspondence using simple two-band models.
3. C. L. Kane and T. C. Lubensky, "Topological boundary modes in isostatic lattices," *Nature Physics* **10**, 39–45 (2014). The foundational paper on topological Maxwell lattices. It introduces the compatibility-matrix winding and its relation to polarized zero modes and states of self-stress.
4. B. G.-g. Chen, N. Upadhyaya, and V. Vitelli, "Nonlinear conduction via solitons in a topological mechanical insulator," *Proceedings of the National Academy of Sciences* **111**, 13004–13009 (2014). A beautiful mechanical realization of SSH-like topology in a rotor chain, emphasizing how an edge zero mode can become a nonlinear soliton.
5. T. C. Lubensky, C. L. Kane, X. Mao, A. Souslov, and K. Sun, "Phonons and elasticity in critically coordinated lattices," *Reports on Progress in Physics* **78**, 073901 (2015). A review of Maxwell counting, zero modes, states of self-stress, and the elasticity of critically coordinated lattices, including topological mechanics.
6. G. Ma, M. Xiao, and C. T. Chan, "Topological phases in acoustic and mechanical systems," *Nature Reviews Physics* **1**, 281–294 (2019). A broad review of topological acoustics and mechanics, including Dirac points, quantum-Hall-like phases, spin-Hall-like phases, valley phases, Floquet phases, and Weyl systems.

## Homework 3: Computing Topological Mechanical Modes

Lecture 3 introduced two related but distinct ideas: SSH-type band topology and Maxwell topology. This homework focuses on quantities that can be computed directly: null vectors of a compatibility matrix, winding numbers, and edge-mode localization.

### Problem 1: A finite rotor chain and its zero mode

Consider an open Maxwell rotor chain with $N$ rotors and $N-1$ linkages. The linearized bond extensions are

$$e_j = c_1\theta_j + c_2\theta_{j+1}, \qquad j = 1, \ldots, N-1. \tag{3.6.9}$$

Equivalently,

$$e = C\theta, \tag{3.6.10}$$

where $C$ is an $(N-1)\times N$ compatibility matrix.

1. Write the matrix elements of $C$ explicitly.
2. For $N = 30$, $c_1 = 0.4$, and $c_2 = 1$, compute a normalized vector in the null space of $C$. Plot $|\theta_j|$ versus $j$.
3. Compare your numerical zero mode with the analytic form

$$\theta_j \propto \left(-\frac{c_1}{c_2}\right)^{j-1}. \tag{3.6.11}$$

   Extract the localization length $\xi$ from

$$|\theta_j| \sim e^{-j/\xi}. \tag{3.6.12}$$

4. Repeat the calculation for $c_1 = 1$ and $c_2 = 0.4$. Where is the zero mode localized? Explain the result using the ratio $|c_1/c_2|$.

### Problem 2: A kagome-style Maxwell winding calculation

A two-dimensional Maxwell lattice, such as a deformed kagome lattice, has a square compatibility matrix $C(k_1, k_2)$ in the bulk. Its topological information can be read from the phase winding of

$$f(k_1, k_2) = \det C(k_1, k_2). \tag{3.6.13}$$

For this problem, use the simplified kagome-style determinant

$$f(k_1, k_2) = c_0 + c_1 e^{ik_1} + c_2 e^{ik_2}, \qquad -\pi < k_1, k_2 \le \pi. \tag{3.6.14}$$

This model is not meant to reproduce all microscopic details of the kagome lattice. It is a compact model for the same Maxwell-topology calculation: the winding of $\det C$.

Consider two parameter sets:

$$\text{Phase A:} \qquad (c_0, c_1, c_2) = (1.4, 0.7, 0.3), \tag{3.6.15}$$

and

$$\text{Phase B:} \qquad (c_0, c_1, c_2) = (1.0, 1.4, 0.3). \tag{3.6.16}$$

1. For each phase, plot the complex curve

$$f(k_1, k_2) \tag{3.6.17}$$

as $k_1$ winds from $-\pi$ to $\pi$, for several fixed values of $k_2$. Does the curve enclose the origin?

2. Compute the winding number

$$\nu_1(k_2) = \frac{1}{2\pi} \int_{-\pi}^{\pi} dk_1 \, \partial_{k_1} \arg f(k_1, k_2). \tag{3.6.18}$$

Numerically, this can be done by unwrapping the phase of $f(k_1, k_2)$ as a function of $k_1$.

3. Similarly compute

$$\nu_2(k_1) = \frac{1}{2\pi} \int_{-\pi}^{\pi} dk_2 \, \partial_{k_2} \arg f(k_1, k_2). \tag{3.6.19}$$

Which phase has nonzero Maxwell polarization? In which lattice direction is it polarized?

4. Now consider an edge normal to the $\mathbf{a}_1$ direction. Replace

$$e^{ik_1} \to z \tag{3.6.20}$$

and solve the zero-mode equation

$$f(z, k_2) = c_0 + c_1 z + c_2 e^{ik_2} = 0. \tag{3.6.21}$$

Show that

$$z(k_2) = -\frac{c_0 + c_2 e^{ik_2}}{c_1}. \tag{3.6.22}$$

A mode localized near the left edge has $|z(k_2)| < 1$. For Phase B, plot $|z(k_2)|$ and the localization length

$$\xi(k_2) = -\frac{1}{\log |z(k_2)|}. \tag{3.6.23}$$

5. In a short paragraph, compare this two-dimensional calculation with the rotor-chain result. What plays the role of $C(k) = c_1 + c_2 e^{ika}$? What new feature appears in two dimensions?